BOREAS An international journal of Quaternary research

Lateglacial and Holocene environmental history of the central Kola region, northwestern Russia revealed by a sediment succession from Lake Imandra

MATTHIAS LENZ, LARISA SAVELIEVA, LARISA FROLOVA, ANNA CHEREZOVA, MATTHIAS MOROS, MARLENE M. BAUMER, RAPHAEL GROMIG, NATALIA KOSTROMINA, NIYAZ NIGMATULLIN, VASILI KOLKA†, BENRD WAGNER, GRIGORY FEDOROV AND MARTIN MELLES

BOREAS

Lenz, M., Savelieva, L., Frolova, L., Cherezova, A., Moros, M., Baumer, M. M., Gromig, R., Kostromina, N., Nigmatullin, N., Kolka, V., Wagner, B., Fedorov, G. & Melles, M.: Lateglacial and Holocene environmental history of the central Kola region, northwestern Russia revealed by a sediment succession from Lake Imandra. *Boreas*. https://doi.org/10.1111/bor.12465. ISSN 0300-9483.

Bolshaya Imandra, the northern sub-basin of Lake Imandra, was investigated by a hydro-acoustic survey followed by sediment coring down to the acoustic basement. The sediment record was analysed by a combined physical, biogeochemical, sedimentological, granulometrical and micropalaeontological approach to reconstruct the regional climatic and environmental history. Chronological control was obtained by ^{14}C dating, ^{137}Cs, and Hg markers as well as pollen stratigraphy and revealed that the sediment succession offers the first continuous record spanning the Lateglacial and Holocene for this lake. Following the deglaciation prior to *c.* 13 200 cal. a BP, the lake's sub-basin initially was occupied by a glacifluvial river system, before a proglacial lake with glaciolacustrine sedimentation established. Rather mild climate, a sparse vegetation cover and successive retreat of the Scandinavian Ice Sheet (SIS) from the lake catchment characterized the Bølling/Allerød interstadial, lasting until 12 710 cal. a BP. During the subsequent Younger Dryas chronozone, until 11 550 cal. a BP, climate cooling led to a decrease in vegetation cover and a re-advance of the SIS. The SIS disappeared from the catchment at the Holocene transition, but small glaciers persisted in the mountains at the eastern lake shore. During the Early Holocene, until 8400 cal. a BP, sedimentation changed from glaciolacustrine to lacustrine and rising temperatures caused the spread of thermophilous vegetation. The Middle Holocene, until 3700 cal. a BP, comprises the regional Holocene Thermal Maximum (8000–4600 cal. a BP) with relatively stable temperatures, denser vegetation cover and absence of mountain glaciers. Reoccurrence of mountain glaciers during the Late Holocene, until 30 cal. a BP, presumably results from a slight cooling and increased humidity. Since *c.* 30 cal. a BP Lake Imandra has been strongly influenced by human impact, originating in industrial and mining activities. Our results are in overall agreement with vegetation and climate reconstructions in the Kola region.

Matthias Lenz (lenzm2@uni-koeln.de), Marlene Baumer, Raphael Gromig, Benrd Wagner and Martin Melles, Institute of Geology and Mineralogy, University of Cologne, Zülpicher Str. 49a, Cologne D-50674, Germany; Larisa Savelieva, St. Petersburg State University, Universitetskaya Nab. 7/9, St. Petersburg 199034, Russia; Larisa Frolova and Niyaz Nigmatullin, Laboratory of Paleoclimatology, Paleoecology, Paleomagnetism, Kazan Federal University, Kremlevskaya Street 18, Kazan 420008, Russia; Anna Cherezova, Karpinski Russian Geological Research Institute, Sredny Prospect 74, St. Petersburg 199106, Russia; Matthias Moros, Leibniz Institute for Baltic Sea Research Warnemünde, Seestrasse 15, Rostock D-18119, Germany; Natalia Kostromina, St. Petersburg State University, Universitetskaya Nab. 7/9, St. Petersburg 199034, Russia and Gramberg All-Russia Scientific Research Institute for Geology and Mineral Resources of the Ocean (VNIIOkeangeologia), Angliyskiy av., 1, St. Petersburg 190121, Russia; Vasili Kolka, Geological Institute of Kola Science Centre RAS, 14 Fersman Street, Apatity 184209, Russia; Grigory Fedorov, St. Petersburg State University, Universitetskaya Nab. 7/9, St. Petersburg 199034, Russia and Arctic and Antarctic Research Institute, Bering Str. 38, St. Petersburg 199397, Russia; *received 28th April 2020, accepted 17th June 2020.* *†Deceased*

Lake Imandra at the southwestern border of the Kola Peninsula (NW Russia) is the largest lake in the Russian part of the European Arctic. However, the lake is located in the most heavily populated arctic region with up to 500 000 people living within the catchment area (Rzevsky 1997; Rumyantsev *et al.* 2012). Anthropogenic landscape transformation since the early AD 1920s has led to significant changes in the water and land ecosystems, which makes this site a prime location to study human impacts vs. a natural background state (Doncheva & Kalutskov 1977; Chidzikov 1980; Moiseenko & Yakovlev 1990; Kravtsova 1995; Innes & Oleksyn 1999; Rigina *et al.* 2000; Moiseenko *et al.* 2002, 2009a, b; Voinov *et al.* 2004; Dauvalter & Kashulin 2015, 2018).

The environmental history prior to the distinct anthropogenic impact has been studied in much less detail. Repeated glaciations of the Kola region throughout the Quaternary were associated with widespread erosion and a poor preservation of lithostratigraphical records (Niemela *et al.* 1993). The available records, therefore, mostly have a limited time range, because they are restricted to the Lateglacial and Holocene times, and poor age control (Davydova & Servant-Vildary 1996; Ilyashuk *et al.* 2013).

During the Last Glacial Maximum (LGM), the Kola region was entirely covered by the Scandinavian Ice Sheet (SIS) (Svendsen *et al.* 2004; Hughes *et al.* 2016; Stroeven *et al.* 2016; Patton *et al.* 2017). On the central part of the peninsula, however, evidence of the LGM ice cover, such as erosional features and moraines, is rare (Lundqvist 1986; Elverhøi *et al.* 1993; Lundqvist & Saarnisto 1995; Kleman *et al.* 1997; Boulton 2001; Stroeven *et al.* 2016), probably as a result of presumably cold-based ice conditions (Kleman & Hättestrand 1999; Kleman &

DOI 10.1111/bor.12465

Glasser 2007). Also the timing of the deglaciation in this region is not well known. A few existing surface exposure dates give maximum ages that have a wide range between 23 and 16 cal. ka BP (Stroeven *et al.* 2016). Consequently, the time of deglaciation until today is based on the interpolation between two prominent end moraines in the Karelian region and their equivalents on the northern shore of the Kola Peninsula (Lundqvist 1986; Ekman *et al.* 1991; Lundqvist & Saarnisto 1995; Rainio *et al.* 1995; Kleman *et al.* 1997; Boulton 2001; Svendsen *et al.* 2004; Demidov *et al.* 2006; Putkinen *et al.* 2011; Hughes *et al.* 2016).

The postglacial history was reconstructed based on investigations of aquatic and terrestrial sedimentary archives. Early investigations focused on the vegetation history derived from pollen analyses, but most studies lack a good temporal resolution and robust chronological control (Armand *et al.* 1969; Malyasova *et al.* 1973, 1974; Kagan *et al.* 1992; Davydova & Servant-Vildary 1996). In more recent studies, age control was improved and the palynological studies were complemented by macrofossil analyses for detailed reconstructions of treeline dynamics (Kremenetski *et al.* 1999; MacDonald *et al.* 2000), and diatom analyses for palaeolimnological reconstructions (Snyder *et al.* 2000; Kremenetski *et al.* 2004; Olyunina *et al.* 2008). In addition, the first multiproxy analyses on lake sediments, including sedimentological and geochemical methods, provided more detailed information concerning the postglacial climatic and environmental history (Solovieva & Jones 2002; Jones *et al.* 2004; Ilyashuk *et al.* 2013). Furthermore, the investigation of marine to lacustrine deposits on land provided insights into Holocene relative sea-level changes, the development of diatom assemblages and the spread of vegetation in the coastal areas of the Kola Peninsula (Snyder *et al.* 1997; Corner *et al.* 1999, 2001; Korsakova *et al.* 2016).

Here we present the first sediment succession from the central part of the Kola region, which reaches back almost continuously to the Bølling/Allerød chronozone in an unprecedented temporal resolution. The 8.46-m-long sediment core Co1410 from the northern sub-basin of Lake Imandra (Fig. 1) was investigated by a multidisciplinary approach using lithological, granulometrical, (bio-) geochemical, geochronological and biological data to reconstruct the environmental and climatic history of the lake and its catchment and to achieve a better understanding of landscape dynamics.

Study area

Lake Imandra is an arctic lake located in the southwestern part of the Kola Peninsula, northwestern Russia (latitude 67°21′–68°04′N, longitude 31°52′–33°27′E; Fig. 1A). The lake has a surface area of 812 km² (880.4 km² including islands), and an indented shoreline of more than 2500 km (Rzevsky 1997; Rumyantsev *et al.* 2012). The catchment area of 12 300 km² equals roughly 15 times the lake surface (Fig. 1B). The relief is relatively flat over large parts of the catchment, with only 8% of the area exceeding 500 m above sea level (m a.s.l.) comprising parts of a mountain range with highest elevations up to 1200 m a.s.l. occurring in the east. The lake is fed by 1379 small tributaries, which partly flow through other smaller lakes. The only outlet is the Niva River, which drains to the south into the Kandalaksha Gulf of the White Sea (Moiseenko & Yakovlev 1990).

The present-day lake is dammed and the lake level is subject to seasonal fluctuations between 126.7 and 128.3 m a.s.l. The lake has average and maximum water depths of 14 and 67 m, respectively, and a volume of ~11 km³ (Elshin & Kupriyanov 1970). Lake Imandra is subdivided into three relatively isolated sub-basins, which are connected only via narrow straits (salmas). Lake Bolshaya Imandra (= Big Imandra) in the north (Fig. 1B – ①) is the main focus of this study. It has a surface area of 311.6 km², a maximum depth of 67 m, and contains, with a volume of 4.6 km³, the largest amount (42.2%) of water (Rumyantsev *et al.* 2012). Lake Ekostrovskaya Imandra in the central part (Fig. 1B – ②), with an area of 352.2 km² and a maximum depth of 42 m, and Lake Babinskaya Imandra in the west (Fig. 1B – ③), with an area of 148.7 km² and a maximum depth of 43.5 m, share the rest of the volume. Bolshaya Imandra, parts of Ekostrovskaya Imandra and the Niva River have a north–south orientation and are located in a deep north–south depression that separates the Kola Peninsula from the continental part of Fennoscandia (Dauvalter *et al.* 1999a). Babinskaya Imandra and the main parts of Ekostrovskaya Imandra, in contrast, have a west–east extension and are considered to be formed by glacial erosion (Herdendorf 1982).

Human-controlled open pit mining, smelters, and power plants led to the pollution of the lake and its catchment over the last century (Kravtsova 1995; Rigina 2002; Voinov *et al.* 2004; Moiseenko *et al.* 2018), which had a strong impact for example on the water chemistry of Lake Imandra (Rigina *et al.* 2000; Moiseenko *et al.* 2002; Dauvalter & Kashulin 2015). Until the early AD 1920s the lake was, in its natural state, an oligotrophic water body typical of arctic regions and characterized by a low ion concentration between 24–30 mg L^{-1}, water transparency of up to 8 m and pH values around 6.4–7.2 (Moiseenko & Yakovlev 1990; Moiseenko *et al.* 2002). From the AD 1920s onward, the lake experienced a rapid phase of eutrophication. The sum of ions rose to up to 82 mg L^{-1}, water transparency decreased down to less than 1 m, the pH shifted to more alkaline values (up to 8.1) and the aquatic habitat changed accordingly (Kravtsova 1995; Moiseenko *et al.* 1996, 2009a; Dauvalter *et al.* 1999b; Rigina 2002). Since the AD 1990s, environmental constraints have helped to improve the water quality. As a result, Lake Imandra has

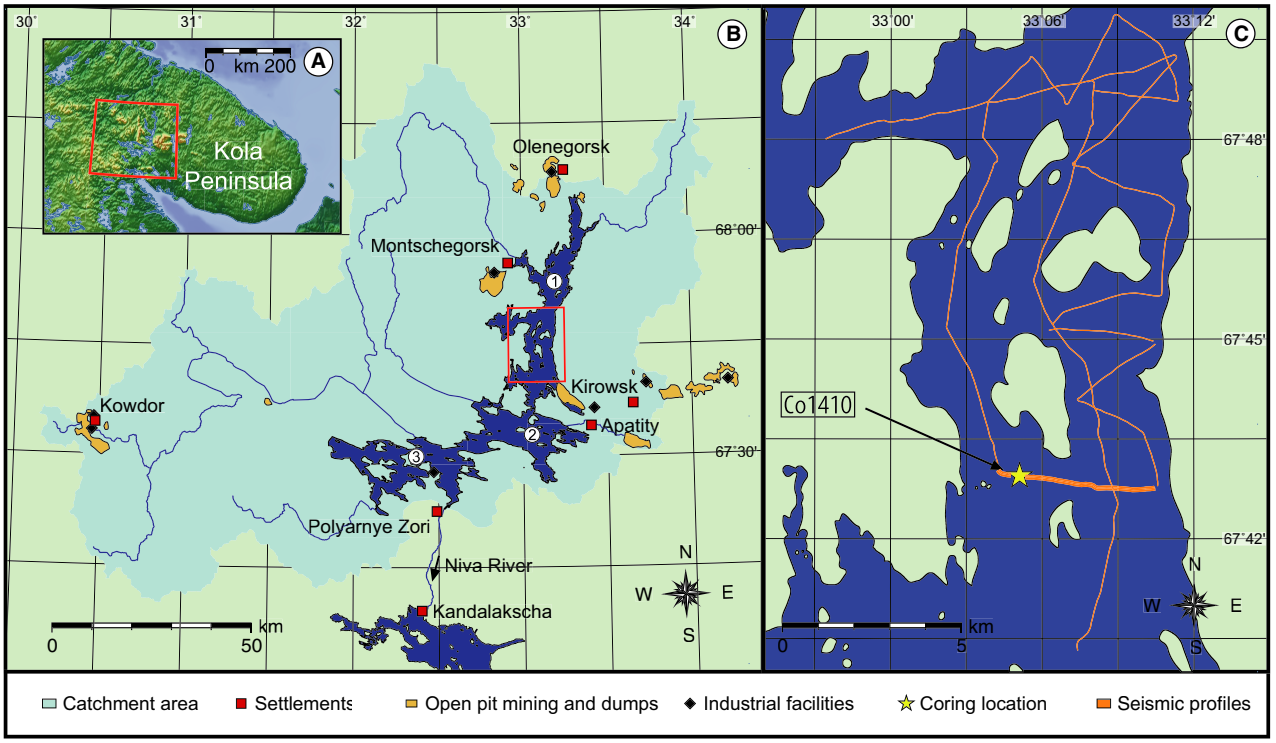

Fig. 1. A. Overview of the location of Lake Imandra in the Kola region in the southwest of Kola Peninsula, Russia (red frame). B. Catchment area of Lake Imandra with settlements larger than 10 000 inhabitants, open pit mines, dumps, and industrial facilities and the three sub-basins ① = Bolshaya/Big Imandra; ② = Ekostrovskaya Imandra; ③ = Babinskaya Imandra. C. Close-up of the middle part of the northern basin of Lake Imandra (see red frame in B) with the coring location (yellow star) and hydro-acoustic profiles (orange lines). The thick orange line highlights the hydro-acoustic profile that is partly shown in Fig. 3.

reached a stable state, with the water transparency increased to several metres and pH values decreased to around 6.4–7.7, but still high ion concentration prevail (Moiseenko *et al.* 2009b, 2018).

The climate at Lake Imandra is a result of the influence of the North Atlantic Current and fairly mild considering its latitudinal position (Rumyantsev *et al.* 2012). Meteorological stations around the lake today record mean annual air temperatures between −0.6 and −1.0 °C, with monthly averaged July and January temperatures of 12.9 and −12.8 °C, respectively, and only 71–74 days per year with temperatures exceeding 10 °C (Zyuzin & Demin 2007; Merkel 2019). Between early November and end of May, Lake Imandra is covered by ice, which reaches thicknesses of 60–90 cm (Elshin & Kupriyanov 1970). The ice cover prevents wind-induced mixing of the water body, resulting in reduced gas exchange with the atmosphere. In April, microbial activity during organic material decomposition partly depletes the oxygen in the bottom waters and at the sediment surface. During the ice-free season wind- and temperature-induced mixing causes widely uniform temperatures throughout the water column (Dauvalter *et al.* 1999a; Ingri *et al.* 2011; Rumyantsev *et al.* 2012). Long-term observations that started in the AD 1960s suggest changes in regional climatic conditions, such as increasing temperatures and decreasing precipitation, which affect the duration of lake-ice cover, the length of the vegetation-growth period, and changes in vegetation (Johansen *et al.* 2005; Demin & Zyuzin 2006; Beck *et al.* 2007; Rubel & Kottek 2010; Ogureeva *et al.* 2012; Høgda *et al.* 2013; Mathisen *et al.* 2014; Marshall *et al.* 2016; Park *et al.* 2016).

The Imandra basin is located in the northern Taiga zone characterized by spruce–birch and pine–birch plant associations (Vasilevskaya 2014). The shorelines today are covered by sub-arctic birch (*Betula pubescens*) and various types of spruce–pine (e.g. *Pinus*) forests with mosses (*Pleurozium schreberi*), dwarf shrubs (*Vaccinium myrtillus* L., *Vaccinium vitis-idea* L., *Vaccinium uliginosum* L., *Empetrum hermaphroditum* Hagerup),= and shrubs (mainly *Betula nana* L., but also *Salix* sp.). Particularly moist conditions result in low heat availability, and hence low evaporation, leading to widespread wetlands (Elshin & Kupriyanov 1970; Zyuzin & Demin 2007). The adjacent Khibiny Mountain massive at the eastern shore, however, exhibits an altitudinal transition in vegetation cover from coniferous forests at lower altitudes towards sub-arctic forests and tundra near the highest elevations (Orlova *et al.* 2012).

The bedrock in the area of Lake Imandra consists of crystalline formations of Archean and Early

Proterozoic age (Fig. 2; Mitrofanov *et al.* 1995). At the northern shores of Bolshaya Imandra, granodiorites of Late Archean age crop out and at the eastern and western shores, sedimentary rocks and volcanic rocks are present, which are mostly covered by Quaternary deposits. The lake basin is also directly connected to the Khibiny Massif in the east, which formed as result of Early Carboniferous intrusions of alkali magma and is uniquely rich in ore deposits and rare-earth elements (Radchenko *et al.* 1994; Pripachkin *et al.* 2013).

Material and methods

Hydro-acoustic survey and coring

In summer 2017, a hydro-acoustic survey was conducted along a total of 80 km of profile lines in the central part of the northern basin of Lake Imandra (Fig. 1C; Bolshaya Imandra). For high-resolution reflection seismic a Micro-GI airgun (2×0.1 L) and a 50-m-long Geometrics GeoEel digital streamer (Geometrics, USA) with 32 channels and a spacing of 1.5625 m was used. Simultaneously, a parametric echo-sounding system (Innomar SES-2000 compact, Germany), operated at 10 kHz, was used. Measurements were conducted from a floating platform (UWITEC, Austria) with an outboard engine using a GPS device with an accuracy of a few metres for navigation. The IHS Kingdom software© version 2016.1 was used for interpretation of the data sets. Depth conversation was conducted assuming a constant seismic velocity of 1430 m s^{-1}.

Based on the hydro-acoustic data, coring site Co1410 was selected at ~23 m water depth (67°42′56.76″N, 33°5′6.42″E, Fig. 1C), where two sediment successions with lengths of 7.98 and 8.65 m, respectively, were recovered only a few metres apart. Coring was conducted from a floating platform using a gravity-corer to retrieve undisturbed near-surface sediments and a percussion piston-corer with a 2-m-long core barrel for deeper sediments (all UWITEC, Austria). After recovery, the core segments were cut into up to 1-m-long sections and kept at low temperatures and in the dark during transport and storage.

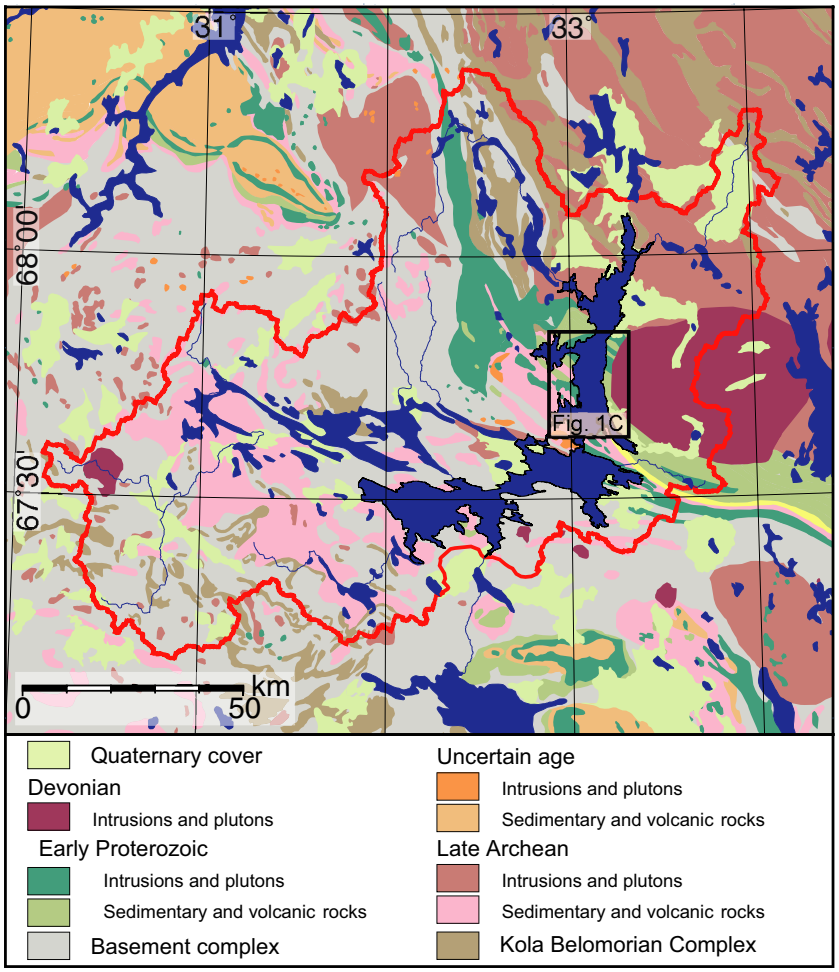

Fig. 2. Simplified geological map of the Lake Imandra area after Mitrofanov *et al.* (2001). The red line marks the lake's catchment area and the black box highlights the study area shown in Fig. 1C.

Core description, XRF-scanning, and development of the core composite

In the laboratories of the University of Cologne, the sediment cores were split lengthwise and the core halves were described for sedimentary structures, grain size (finger probe), colour (Munsell Soil Colour Chart), consistency, carbonate content (reaction with hydrochloric acid (HCl)) and sediment composition (smear-slide microscopy). While one core half was stored as an archive, the working half was used for non-destructive magnetic susceptibility (MS) measurements at a resolution of 1 mm using a multi-sensor core logger (MSCL) equipped with a Bartington MS2E point sensor (Geotek 2016). High-resolution line-scan photography and subsequent X-ray fluorescence (XRF) scanning were carried out at 2-mm resolution with an ITRAX core scanner (Cox Analytical Systems, Sweden), equipped with a Cr-tube and a Si-drift detector in combination with a multi-channel analyser. Voltage and amperage were set to 30 kV and 55 mA, respectively, and the exposure time to 20 s. Prior to the measurement, the sediment surface was carefully flattened and covered with an Ultra-Polyester® thin-film (1.5 μm) (Chemplex, USA). The detected peak area intensities are given in total counts per second (cps) and can be used as semi-quantitative estimates of relative concentrations of the detected elements (Croudace *et al.* 2006). Post-processing of the data was conducted using the QSpec 6.5 software (Cox Analytical Systems, Sweden). Compared to wave dispersive XRF analyses (WD-XRF), XRF scanning is less time consuming, but more susceptible to inaccuracies resulting from variations in the sediment's water content, surface structure, grain size, and porosity (Tjallingii *et al.* 2007; Hennekam & de Lange 2012) as well as a matrix effect, which has a greater impact on the data as organic matter (OM) content increases (Bertin 1975; Beckhoff *et al.* 2006). In order to compensate for these inaccuracies, the data are standardized to the element aluminium (Al), which is most suitable considering its geochemical behaviour (Löwemark *et al.* 2011).

Based on line-scan images, core description, and selected XRF data (Ca counts and Si/Ti ratio) the core segments were merged using the Corelyzer 2.0.4 software (National Lacustrine Core Facility LacCore and Continental Scientific Drilling Coordination Office, CSDCO). All depths refer to the spliced 8.46-m-long master record. A gap between 6.92 and 7.54 m results from missing recovery caused by technical problems.

Subsampling and sedimentological analyses

The core composite Co1410 was continuously subsampled in 2-cm sections. Subsamples were freeze-dried and water content was calculated from the weight loss after freeze-drying. Subsequently, aliquots were taken for biogeochemical, granulometric and palynological analyses.

For biogeochemical analyses, aliquots of 0.5 g were ground to <63 μm and homogenized in a planetary mill (Fritsch, Germany). Bulk sediment concentrations of total nitrogen (TN) and total sulphur (TS) were determined using a Vario Micro Cube combustion CNS elemental analyser (Elementar Analysensysteme GmbH, Germany), whereas total carbon (TC) as well as total inorganic carbon (TIC) were measured using a DIMATOC 2000 (Dimatec Analysentechnik GmbH, Germany). Total organic carbon (TOC) was calculated from the difference between TIC and TC.

For grain-size analyses of the lithogenic material, aliquots of 1.5 g were treated with 15% hydrogen peroxide (H_2O_2), 10% HCl and 1 M sodium hydroxide (NaOH), in order to remove organic material, calcium carbonate and biogenic silica, respectively (Gee *et al.* 2002). The pretreated samples were then dispersed in a solution of about 60 mL deionized water with 1.2 g of sodium pyrophosphate ($Na_4P_2O_7$, 2.5 g L^{-1}, Graham's salt), using a shaker for at least 12 h. The grain-size distribution of the remaining material was determined in three parallel runs with a laser diffraction particle size analyser LS 13 320 (Beckman Coulter GmbH, Germany), which was equipped with an aqueous liquid module (ALM) and an auto prep station (APS).

Statistical analyses

Processing of the grain-size data was carried out with the GRADISTATv8 software (Blott & Pye 2001) based on averaged grain-size distributions of a triplicate measurement of each sample and the method by Folk & Ward (1957). On the processed data end-member modelling was carried out using the AnalySize algorithm (Paterson *et al.* 2016) run with the MatLab software (The MathWorks Inc. 2019).

Multivariate principal component analysis (PCA) was applied to selected XRF (Si, P, K, Ca, Ti, Mn, Fe, Rb, Sr, Zr, Si/Ti, Fe/Mn and Rb/Sr), biogeochemical (TN, TOC and TS) and end-member (EM1, EM2 and EM3) data, in order to create comparable data sets for different sections of the core composite and to explore the grouping of subsamples according to their similarities (Zitko 1994; Jolliffe 2002; Bro & Smilde 2014). PCA was performed using the Palaeontological Statistics (PAST3 v. 3.25) software (Hammer *et al.* 2001).

Pollen analysis

Pollen analyses were carried out at the St. Petersburg State University, Russia. Pollen and spores were extracted from 87 samples with 8–10 cm spacing in the upper part (0–5.16 m) and 2–4 cm in the lower part (5.16–7.82 m) of core Co1410. Analyses followed stan-

dard protocols (Savelieva *et al.* 2019), which included sample preparation with HCl, NaOH and hydrofluoric acid (HF) (Berglund *et al.* 1986), before they were mounted with glycerol on slides. In each sample between 70 and 600 terrestrial pollen grains were counted and identified using a stereomicroscope at 400× magnification. Taxonomic identifications followed Kupriyanova & Alyoshina (1972), Kupriyanova & Alyoshina (1978), Moore *et al.* (1991), Savelieva *et al.* (2013) and the modern pollen reference collection of the St. Petersburg State University. Calculated pollen percentages refer to the total sum of terrestrial pollen. Spore percentages are based on the sum of pollen and spores. *Lycopodium* tablets were used to determine pollen taxa concentrations (Stockmarr 1971).

Cladocera analysis

Sediment samples were prepared for cladoceran analyses at the Kazan Federal University, Russia using the methods described in Korhola & Rautio (2001). In total, 43 samples with a spacing of 2 cm in the upper 0.50 m and 4–14 cm down to 5.10 m were analysed. No samples have been analysed in the lowermost part of the core between 5.10 and 8.45 m. Each sample (0.5–0.6 g of dry sediment) was heated for approximately 30 min at 75 °C in 10% potassium hydroxide (KOH). In the next step the pretreated sediment mixture was sieved using a 50-μm mesh size. The sediment retained on the sieve was transferred with distilled water into a small 12.5-mL vial. A few drops of ethanol (C_2H_6O) and safranin-glycerine solution were added to prevent fungal growth and to stain the cladoceran remains. The chitinous remains of cladocerans (i.e. headshields, shells, postabdomens, postabdomenal claws, and ephippia) were identified with reference to subfossil (Frey 1959, 1973; Szeroczyńska & Sarmaja-Korjonen 2007) and modern (Flößner 2000; Kotov *et al.* 2010) cladoceran identification keys, and their nomenclature follows Kotov *et al.* (2010). The most abundant body part of each species was chosen to represent the number of individuals. Each sample contained between 221 and 294 individuals, from which the percentages for all cladoceran taxa were calculated.

Chronostratigraphical analyses

In order to identify the time markers AD 1900 and AD 1986, according to the event-stratigraphical approach used for nearby Baltic Sea sediments (Moros *et al.* 2017), mercury (Hg) and radionuclide measurements were carried out at the Leibniz Institute for Baltic Sea Research in Warnemünde (IOW), Germany. The activities of artificial ^{137}Cs radionuclides were measured by gamma spectrometry with a CANBERRA BE3830 broad energy Germanium detector (Moros *et al.* 2017). Mercury measurements (Leipe *et al.* 2013) were carried out on subsamples between 20 and 100 mg with a DMA-80 analyser (MLS Company).

Moreover, radiocarbon (^{14}C) dating on organic macro-remains was carried out on 12 samples. Wherever applicable, macro-remains were directly sampled from the sediment core after core opening and during subsampling. In most cases, however, they had to be isolated from subsamples of 1–4 g, which were sieved using mesh widths of 125, 63 and 36 μm. In the isolated fractions, larger organic remains were picked out by hand and smaller ones isolated by density separation. For the latter, a heavy-density solution consisting of sodium polytungstate (calibrated to 2.3 g cm^{-3}) was added to the samples. After 15 min of centrifugation at 2500 rpm, the lighter material floating at the top was pipetted off the solution. This step was repeated three times. Finally, the extracted material was rinsed using deionized water to remove and dissolve any residual sodium polytungstate. The isolated bulk organic and terrestrial plant remains were treated according to the standard protocol of organic material pretreatment of organic material and graphitization (Rethemeyer *et al.* 2013). Samples were measured by accelerator mass spectrometry (AMS) using the radiocarbon dating method of the Cologne-AMS centre (Dewald *et al.* 2013).

For the age-depth model a Bayesian-model approach was employed. In the upper part tie points from the sediment–water interface, ^{137}Cs and Hg measurements, and radiocarbon dating were included in the age-depth model. In the lower part, two tie points were derived for the Bølling/Allerød to Younger Dryas and for the Younger Dryas to Holocene boundaries according to Lohne *et al.* (2013), which are clearly reflected by the palynological data of core Co1410 (see below). The age-depth calculation was performed using the 'rBacon' library (Blaauw & Christen 2011; Blaauw *et al.* 2020) for R (R Development Core Team 2019). The software calibrates radiocarbon dates to calendar years before present (AD 1950) using the IntCal13 calibration curve for terrestrial Northern Hemisphere material (Reimer *et al.* 2013a, b), while negative ^{14}C dates (modern/post-bomb) are calibrated by the NH1 post-bomb calibration curve for the Northern Hemisphere (Hua *et al.* 2013), all with an uncertainty range of 2σ. Pollen-derived ages were calculated with an estimated error of ±100 a, whereas the ^{137}Cs and Hg markers, and the sediment surface were calculated with errors of ±10 a and ±1 a, respectively.

The model was calculated by adding two boundaries (at 0.32 and 5.16 m), where prominent lithological changes suggest the memory of the age-depth calculation should be reset. Moreover, two mass movement deposits (6.50–6.70 and 7.92–8.46 m) were included with an infinite sedimentation rate. Additionally, paying attention to a prominent change in the lithology below 5.16 m, the accumulation mean and shape were adopted to a more rapid sediment accumulation. Based on the computed age-depth model the sedimentation rate was

estimated for those parts of the core that suggest a continuous sedimentation, using the same software package. The probability range was reduced in order to avoid unrealistically high or low sedimentation rate estimates.

Results and discussion

Sediment architecture

Sediments in the vicinity of the coring location Co1410 are characterized by a rather even reflector marking the sediment–water interface, but more rugged sub-bottom reflectors (Fig. 3). The top of the diffuse blue reflector marks the acoustic basement, which occurs at a depth of ~8 m below lake floor at site Co1410 and was penetrated by the sediment corer by about 0.5 m. The blue reflector shows short-distance relief changes in the order of 1–2 m in the surrounding ~100 m, but higher-amplitude changes of about 10 m beyond. The basement is overlain by a subparallel sediment unit of 2.0–2.5 m thickness that is acoustically stratified in more flat areas and widely transparent in steeper areas. This unit is bordered at the top by a strong acoustic impedance contrast (green reflector), which indicates sediments with lower densities above. These sediments are acoustically less stratified, with faint stratification visible in areas with a rather flat green reflector, but massive internal structure in areas with a steeper green reflector. Furthermore, the sediments differ from the underlying sediments by distinct thinning in the areas where the blue and green reflectors are elevated, leading to a strongly reduced relief at their top (reflector 3). Hence, sedimentation between the green and orange reflectors was predominant in depressions and widely levelled the lake floor around the coring site. The orange reflector finally is draped by a thin (<0.5 m) layer of acoustically transparent sediments, bordered by the modern lake floor (red reflector) in a water depth of ~23 m at coring site Co1410.

Lithostratigraphy and biogeochemistry

Based on the visual core description as well as the grain-size, XRF, and water content data the 8.46-m-long core composite Co1410 was subdivided into four main sediment units (I–IV), some of which are composed of subunits (Fig. 4).

Unit I (8.46–7.85 m) – glacifluvial deposition. – The lowermost part of the core consists of lithogenic sediments, with particle sizes varying between silt and very coarse gravel (Fig. 4). The diverse, partly very coarse grain size excluded representative XRF-scanning (Croudace *et al.* 2006) and water content determination and the almost pure lithogenic composition prevented elemental and micropalaeontological analyses (Figs 4, 5). Hence, the genetic interpretation of this sediment unit mainly relies on the core description, the shape of macroscopic grains and the hydro-acoustic characteristics.

The top of Unit I corresponds to the blue reflector, which marks the acoustic basement (Fig. 2). This is explained by the almost pure lithogenic composition and rather coarse grain size of Unit I. The lack of acoustically stratified sediments underneath suggests that Unit I either is rather thick or bordered at the base by impenetrable material such as glacial till or bedrock. In the latter cases, Unit I would most likely represent initial glacifluvial deposition that formed during the deglaciation of the basin. A glacifluvial formation of Unit I is supported by the scarcity of OM and the absence of clay. The latter excludes other depositional processes or formations such as a debrisflow or till. Moreover, the grain-size distribution from silt to gravel indicates a highly variable fluvial transport energy and likely redeposition of glacially supplied material.

Further evidence pointing to a glacifluvial deposition is provided by the shape and composition of the material, which indicate different transport distance and provenance, respectively. Angular nepheline syenites represent a proximal sediment supply to the coring site from the adjacent Khibiny Mountains at the eastern shore (Mitrofanov *et al.* 1995; Mitrofanov & Zozulya 2002), whereas subangular to rounded granodiorites as well as other magmatic and sedimentary rocks indicate a more distal sediment supply from the west (Fig. 2; Radchenko *et al.* 1994; Slabunov *et al.* 2006). A glacifluvial deposition is also supported by the different appearance of the boundaries of sedimentary units I and II in the two sediment cores, recovered just a few metres apart at site Co1410 (Fig. 6). Whilst one core exhibits a very sharp boundary between gravelly sand of Unit I and clayey silt of Unit II, the other core shows a more gradual transition, with a distinct fining upward succession over a few decimetres.

Unit II (7.85–5.16 m) – glaciolacustrine deposition. – Most parts of Unit II comprise laminated sediments, which are characterized by thin (3–35 mm) interbedding of grey silty fine sand and almost pure light greenish-grey clay. These rhythmic layers are interpreted as clastic varves, which were deposited as glaciolacustrine sediments in a proglacial lake. Some coarse-grained, gravel-sized particles, which are sporadically present in the sediment, probably represent ice-rafted debris. A high concentration of lithogenic material is indicated by elevated Ti/Al and K/Al ratios (Fig. 4; Kylander *et al.* 2011).

The absence of bioturbation is further evidence of clastic varve deposition during most of Unit II (e.g. Gromig *et al.* 2019). This also includes hostile conditions for endobenthic organisms, probably due to light limitation by lake-ice and snow cover during winter and to a high suspension load of the lake water in summer, and a

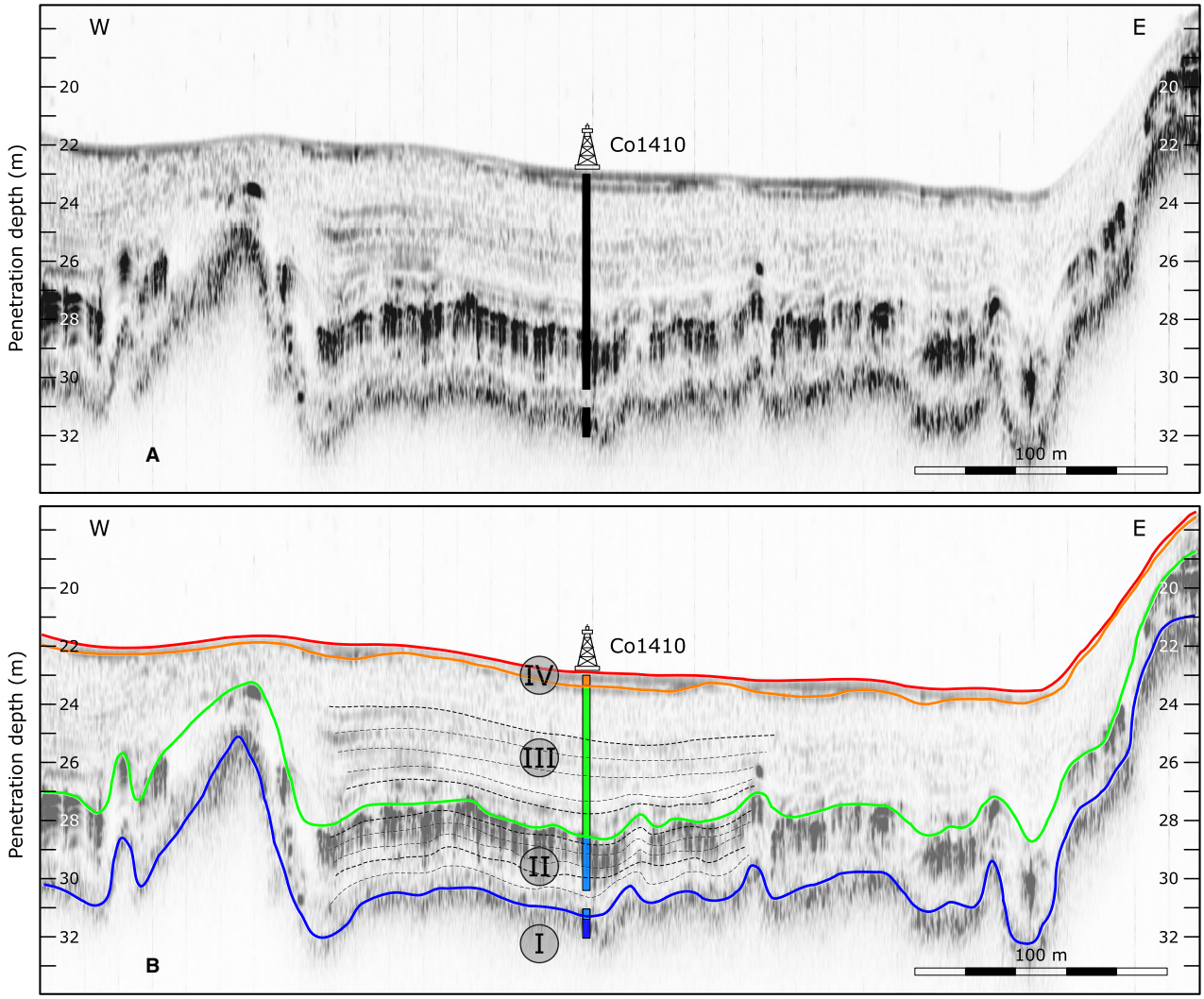

Fig. 3. Un-interpreted (A) and interpreted (B) hydro-acoustic profile crossing the coring position (for location see yellow star in Fig. 1). The scales on both sides give the penetration depths of the hydro-acoustic signal below lake surface according to a seismic velocity of 1430 m s^{-1}. The bar below the coring tower indicates the sediment recovery from site Co1410, with the different colours reflecting the sediment units I–IV defined in Fig. 4.

very low concentration of nutrients. The latter is indicated by the absence of terrestrial or aquatic macrophyte remains and very low amounts of finely dispersed OM, as revealed by the lowest recorded TOC (<0.2%) and TS (<0.02%) values of the sediment succession Co1410 (Fig. 4). Strong fluctuations in the TOC/TN ratio (2–27) suggest that OM experienced repeated and short-term changes in the proportions of terrestrial and aquatic sources (Meyers *et al.* 1995), and distinct decomposition. Pollen grains contribute to terrestrial OM supply; however, their low total concentration (<10 000 pollen grains g^{-1}) and low arboreal pollen (AP) to non-arboreal pollen (NAP) ratio (Fig. 5) indicate a sparse, herb-dominated vegetation cover of the landscape (Favre *et al.* 2008).

Throughout the clastic varve deposition of Unit II, differences in sediment composition reflect some gradual changes in the environmental conditions. Sediments of Subunit IIa are rather coarse-grained deposits, also reflected by low Rb/Sr ratios and EM1, which reflect a low clay and fine silt content. Medium silt or coarse silt and sand are represented by high Zr/Rb and EM2 or EM3, respectively (Figs 4, 7; Kalugin *et al.* 2007; Kylander *et al.* 2011). Rather high EM1 and EM2 as well as low EM3 might be associated with a high meltwater supply, which may occur in the proximity of a retreating ice sheet. A relatively high amount of *Pinus* pollen along with an enhanced AP/NAP ratio especially in the lower part of the Subunit (Fig. 5), might be a consequence of aeolian transport.

In Subunit IIb, between 6.70 and 6.50 m, the clastic varve deposition is interrupted by dark and massive, well-sorted coarse silt to fine sand (Fig. 4). As a consequence of the high proportion of coarse sediments,

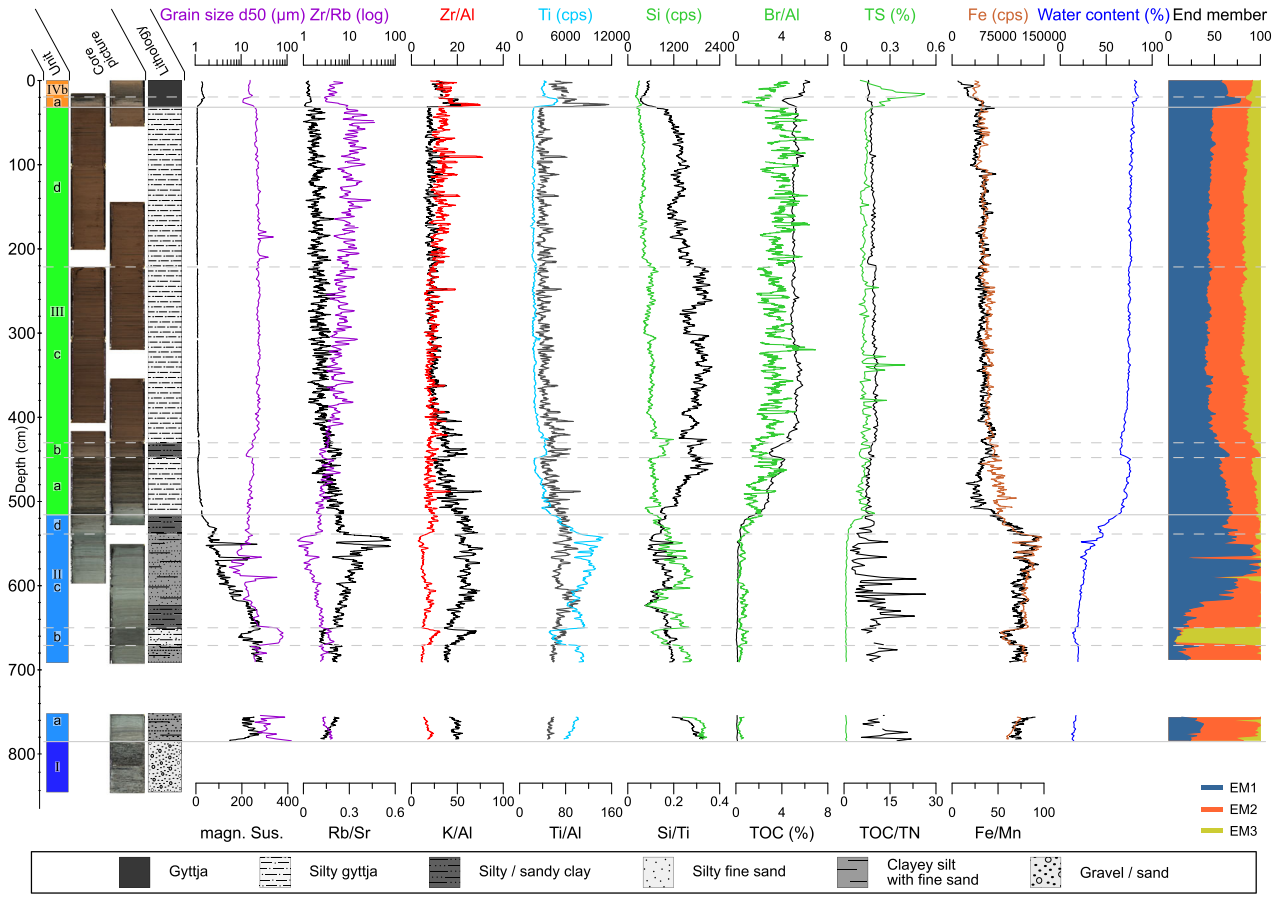

Fig. 4. Lithological units, core pictures and lithology of core Co1410, next to the sedimentary proxies grain size d50 (purple line), magnetic susceptibility, Zr/Rb ratio (purple line), Rb/Sr ratio, Zr/Al ratio (red line), K/Al ratio, Ti counts (blue line), Ti/Al ratio, Si counts (green line), Si/Ti ratio, Br/Al ratio (green line), TOC content, TS content (green line), TOC/TN ratio, Fe counts (brown line), Fe/Mn ratio, water content (blue line) and end-member portions (blue = EM1; orange = EM2; yellow = EM3).

this Subunit is demarcated from the other Subunits in the PCA (Fig. 7). It is also displayed in the hydro-acoustic profile as an acoustically transparent layer about 1 m above the blue reflector (Fig. 3), indicating its origin in a mass movement process (Lebas *et al.* 2019). The formation of this Subunit by a mass movement event is supported by a sharp, likely erosive lower and transitional upper boundary. The most probable mechanism of sediment deposition is a grain flow of pre-sorted sediment, for instance originating from a delta (Sauerbrey *et al.* 2013).

In the lowermost part of Subunit IIc, decreasing EM2 and medium silt contents at the expense of increasing EM1 values (Figs 4, 7) are probably attributed to a persisting proximity of the ice margin. Moreover, a broad increase in *Artemisia* pollen (Fig. 5) suggests that a sparse, herb-dominated vegetation established in a glacial setting. In the middle part of Subunit IIc, highest input of fine-grained material as reflected in EM1, Rb/Sr ratios and water content (Håkanson 1977; Kalugin *et al.* 2007; Kylander *et al.* 2011), indicates an initially high glacial meltwater supply, whereas in the upper part of Subunit IIc decreasing EM1 and Rb/Sr ratios suggest a decrease in transport energy, probably as a result of glacier retreat (Fig. 4). This is supported by a decreasing mean grain size (d50), MS, EM3, Zr/Rb ratios (Peck *et al.* 1994; Cohen 2003; Reynolds *et al.* 2004) and gradual decrease in varve thickness over the course of the upper part of Subunit IIc. Furthermore, a simultaneous decrease of *Artemisia* pollen indicates less favourable conditions for the growth of herbs (Fig. 5).

During deposition of Subunit IId, the grain-size spectrum shows a slightly coarser composition and little variation, as reflected in the grain-size end members as well as the Rb/Sr and Zr/Rb ratios (Fig. 4). This is likely attributed to elevated but rather constant meltwater supply from glaciers. A decreasing amount of *Artemisia* pollen (Fig. 5) indicates more favourable growing conditions for the vegetation in the catchment and a slight increase in the total pollen concentration (Fig. 5) probably points to lower sedimentation rates (Fig. 8). This correlates with the distinctly increasing biogenic accumulation at the expense of the lithogenic sediment

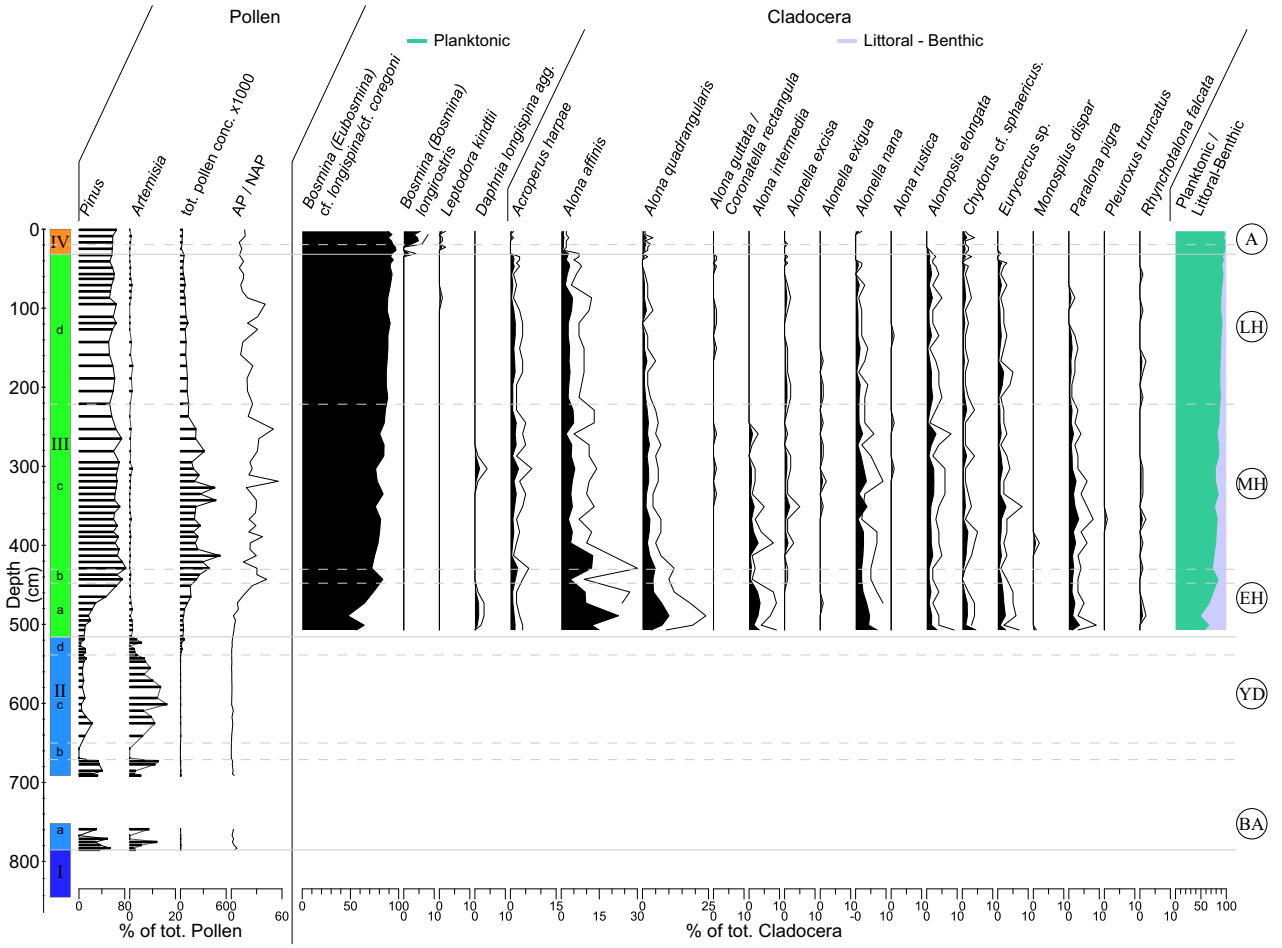

Fig. 5. Lithological units, selected pollen and selected, so far analysed, cladoceran data of core Co1410. Note the different scales for pollen and cladocerans. Each bar in the pollen section of the diagram represents one analysed sample. Percentages of total cladocerans are represented by the black areas, whereas the black lines show the single counts of each taxon. Circles on the right represent chronozones (BA = Bølling/Allerød; YD = Younger Dryas; EH = Early Holocene; MH = Middle Holocene; LH = Late Holocene; A = anthropogenic influence).

supply, reflected by increasing TOC and TS values and decreasing Ti/Al and K/Al ratios (Figs 4, 7).

Unit III (5.16–0.32 m) – lacustrine deposition. – The impedance contrast of the green acoustic reflector (Fig. 3), marking the boundary between higher densities of Unit II and lower densities of Unit III, is predominantly controlled by a further increase in biogenic accumulation, rather than by grain size, which remains relatively constant at the transition. Higher OM accumulation is reflected by a higher TOC (~6%) and TS (~0.4%) in Unit III, along with lower Ti/Al and K/Al ratios (Fig. 4) and higher pollen concentrations (up to 530 000 pollen grains g^{-1}; Fig. 5). Enhanced productivity in Unit III is confirmed by higher Br/Al ratios, as a result of the capacity of Br to be independent of matrix effects and to form strong covalent bonds with organic molecules (Davies *et al.* 2015). Furthermore, significantly higher Si/Ti ratios along with constant Si counts suggest a higher in-lake productivity of diatoms (Brown *et al.* 2007; Melles *et al.* 2012), which is confirmed by a high abundance of diatoms in the microscopic smear slides.

The increased biogenic accumulation along with decreased lithogenic sediment supply during the deposition of Unit III indicates lacustrine conditions in the absence of a significant sediment supply from glaciers in the catchment. Brownish sediment colours and low Fe/Mn ratios suggest complete oxygenation of the water column (Fig. 4; Cuven *et al.* 2011). The appearance of varying amounts of dark brown to black streaks is related to reducing conditions of soils in the catchment. This is derived from an anti-correlation of Fe/Mn ratios and Fe count peaks, most obvious in the lower part of the unit (Fig. 4), which results from the leaching of Mn in the soils and formation of the black manganese oxides (e.g. MnO_2) in the lake under oxygenated bottom-water conditions (Mackereth 1966; Engstrom & Wright 1984; Renberg 1985; Bryant *et al.* 1997).

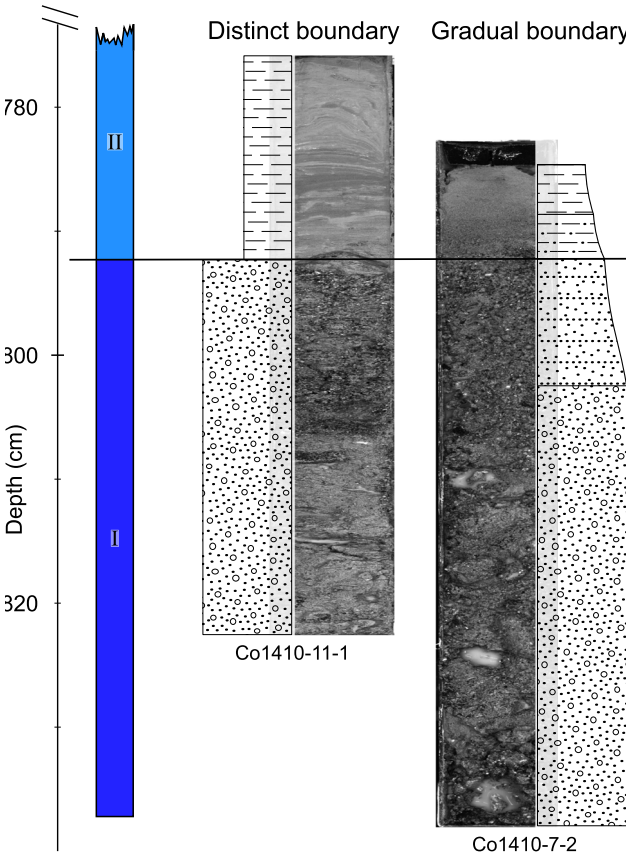

Fig. 6. Sharp (left) and gradual (right) transitions between Unit I and Unit II in the two parallel cores, which were recovered only a few metres apart from each other at site Co1410.

Throughout Unit III, the strongest changes in sediment composition occur in Subunit IIIa. There, all proxies indicating biogenic productivity (TOC, S, Br/Al, Si/TI, pollen and diatoms) show strong increases. This reflects an increase in biogenic accumulation, which according to simultaneously slightly increasing TOC/TN ratios originates from terrestrial rather than from lacustrine OM (Meyers *et al.* 1995; Silliman *et al.* 1996). Within the pollen assemblages, an increase in *Pinus* pollen at the expense of *Artemisia* pollen along with an increase in the AP/NAP ratio (Fig. 5) indicate the emergence of a tree-prevalent landscape (Favre *et al.* 2008). Coarser grain sizes (Figs 4, 7) suggest an increased transport energy, although the decrease in the relative amount of lithogenic sediment supply, as reflected in reduced K/Al and Ti/Al ratios, can be attributed to increased soil stabilization. The cladoceran littoral-benthic chydorid assemblages, which comprise *Alona affinis*, *Alona quadrangularis*, *Alonella nana* and *Alona intermedia*, suggest the prevalence of relatively cool waters (Harmsworth 1968; Whiteside 1970; Korhola & Rautio 2001; Sarmaja-Korjonen 2002; Nevalainen *et al.* 2015; Bledzki & Rybak 2016). Indications for a fresh, oligotrophic water body come from the presence of the dominant taxa *Bosmina* (*Eubosmina*) cf. *longispina*/cf. *coregoni* and *Alona affinis* as well as a low taxa diversity (Hofmann 1996). A low planktonic/littoral-benthic ratio of the cladocerans (Fig. 5), in particular in the lower part of Subunit IIIa, reveals widespread areas with shallower water depth, which likely are attributed to a low lake-level. This explains well the sediment becoming concentrated in deeper parts of the lake, which is evident in hydro-acoustic profiles for the lower part of Unit III (Fig. 3).

Subunit IIIb, which corresponds to an acoustically transparent layer at ~4.50 m at coring site Co1410 (Fig. 3), differs from Subunit IIIa by a lighter sediment colour and reduced occurrence of dark streaks. Lithogenic sediment supply, according to elevated Ti/Al and K/Al ratios, is slightly increased, whereas biogenic sedimentation, as revealed by lowered TOC and Br/Al values, is reduced (Figs 4, 7). A slight decrease in *Pinus* pollen as well as a distinct increase in the Cladocera *Alona affinis* towards the top of Subunit IIIb is likely attributed to less favourable conditions for vegetation growth and more favourable for cold-adapted cladocerans (Kattel & Sirocko 2011).

Subunit IIIc shows low Ti/Al and K/Al values, and a high level of organic deposition, predominantly reflected in high TOC and Si/Ti values (Figs 4, 7). This indicates reduced lithogenic sediment supply, which is supported by a denser vegetation cover in the catchment, as inferred from highest abundances of *Pinus* pollen, total pollen concentration, and AP/NAP ratios in the sediment record Co1410 (Fig. 5). A distinct decrease in the fine fraction, represented by EM1 (Figs 4, 7), may be associated with a strongly reduced glacial meltwater supply. The appearance of *Alonella exigua* and *Alona guttata*/*Coronatella rectangula* (Sarmaja-Korjonen *et al.* 2003; Nevalainen *et al.* 2013) as well as the appearance of *Alonella excisa*, *Alona rustica* and *Pleuroxus truncatus* (Hann & Warner 1987) and the decrease of *Alona intermedia* and *Alonella nana* (Nevalainen *et al.* 2013) indicate favourable conditions for cladoceran development, which allowed for the appearance of many new taxa and maximal cladoceran species diversity (Hofmann 1987).

Subunit IIId shows only small differences to Subunit IIIc. Slightly reduced Si/Ti ratios can be at least partly explained by reduced Si concentrations (Fig. 4) and indicate lower aquatic productivity or slightly increased input of lithogenic material (Fig. 7). The latter is supported by a slight decrease of *Pinus* pollen, AP/NAP ratios, and total pollen concentration (Fig. 5), and increasing Zr/Rb and Zr/Al ratios, which indicate enhanced aeolian supply (Müller *et al.* 2001). However, an elevated Br/Al ratio (Mayer *et al.* 2007; Ziegler *et al.* 2008), and a decrease in the TOC/TN ratio suggest higher aquatic productivity or a reduced terrestrial OM supply.

Unit IV (0.32–0.00 m) – lacustrine deposition. – A prominent change in sediment colour and geochemical

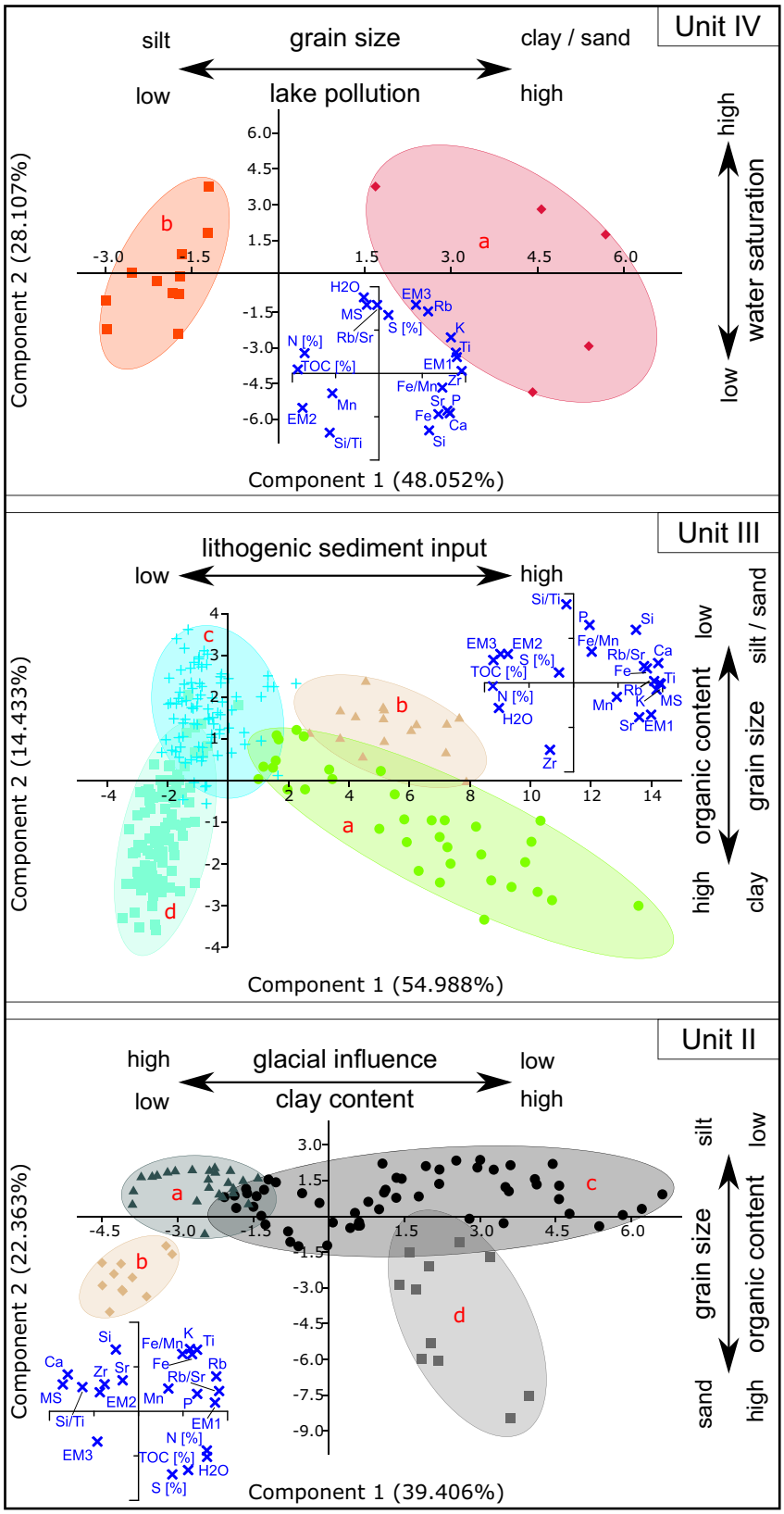

Fig. 7. PCAs of Units II, III and IV showing different trends in response to changing environmental conditions and processes based upon geochemical data and grain-size distributions. Scatterplots of loading 1 (*x*-axis) vs. loading 2 (*y*-axis) are shown in the small plots in blue colour for each unit and the significances of component 1 (*x*-axis) and component 2 (*y*-axis) are specified for each unit.

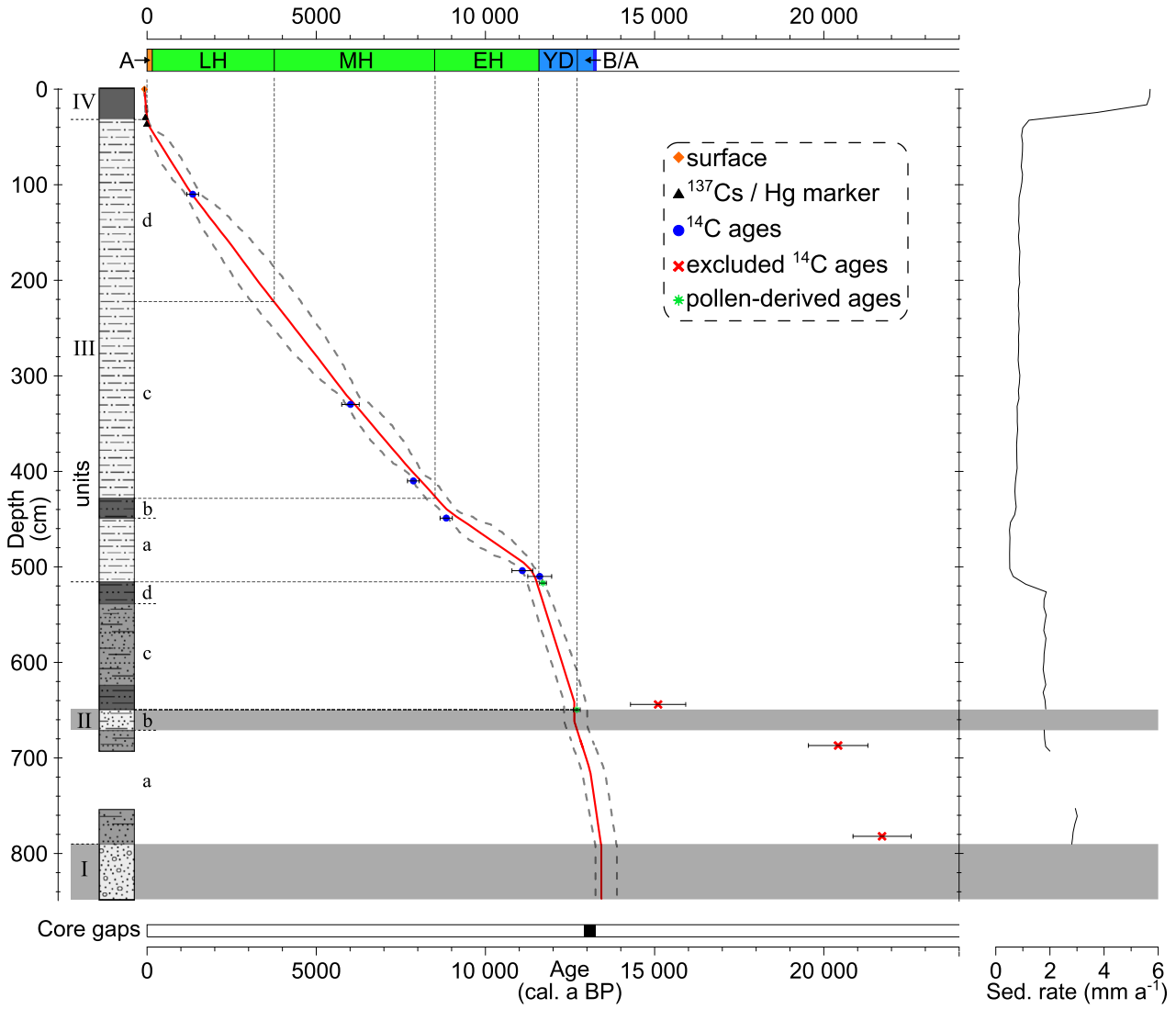

Fig. 8. Age-depth model of core Co1410, based on six ^{14}C ages derived from organic macro-remains and additional tie points from ^{137}Cs and Hg measurements as well as pollen stratigraphy with the upper and lower boundary of the Younger Dryas according to Lohne *et al.* (2013) for northern Europe. ^{14}C ages obtained from the lower part of the core have been excluded from the age-depth calculation (see Results and discussion). The sedimentation rate displayed on the right was calculated from the Bayesian age-depth model. The upper bar shows the stratigraphical framework of the study. B/A = Bølling/Allerød; YD = Younger Dryas; EH = Early Holocene; MH = Middle Holocene; LH = Late Holocene; A = anthropogenic influence. The black rectangle in the bar at the bottom indicates the period not reflected by the core as a result of a core gap between 6.92 and 7.54 m.

composition is visible at the transition to sediments of Unit IV, and is also reflected in the low-impedance orange reflector close to the lake floor (Fig. 3). Despite its low thickness of only 0.32 m at coring site Co1410, Unit IV can clearly be divided into two Subunits of different composition and genesis.

Unit IVa consists of massive light olive grey, silty clay. Pronounced increases of MS and EM1 values, Ti/Al and K/Al ratios, and Ti counts (Figs 4, 7) are attributed to enhanced input of lithogenic material of particularly fine grain size. The constant occurrence of the Cladocera *Chydorus* spp., which is the most toxic-tolerant taxon, in combination with the disappearance of e.g. *Alonopsis elongata* and the appearance of *Leptodora kindtii*, indicates a high degree of eutrophication (Nevalainen *et al.* 2013, 2015). The disappearance of the cladocerans *Alona affinis* and *Acroperus harpae*, as indicators for cold-water and sub-arctic conditions (Harmsworth 1968), may reflect rising temperatures in the water body. Significantly reduced Si/Ti and Br/Al ratios as well as TOC values are probably ascribed to dilution effects as a result of enhanced lithogenic input (Leng *et al.* 2012); however, they might also reflect a decrease in biogenic accumulation.

Compared to the distinct transition at the lower boundary of Subunit IVa, its change to Subunit IVb is

more gradual. Subunit IVb covers the topmost 0.20 m of core Co1410 and is characterized by greyish brown to light olive brown, massive to weakly stratified organic mud. Most proxies change in the direction of Unit III values, thus suggesting a modification of the lake's ecosystem. For instance, somewhat decreasing values of MS, EM1, Ti/Al, K/Al and Ti counts in Subunit IVb, simultaneous with increasing grain size d50 and EM2 (Figs 4, 7), suggest lower input of fine-grained lithogenic sediment from the catchment. Additionally, aeolian input probably became reduced, as suggested by a decrease in Zr/Al (Fig. 4). Increasing TOC and Si/Ti point to a decreasing influence of lithogenic dilution, but may also represent an increase in in-lake bioproductivity. This may have caused short-term oxygen depletion of the bottom water, as indicated by a distinct peak in TS (Fig. 4). Persistent eutrophication is indicated by the replacement of Cladocera *Bosmina* (*Eubosmina*) by Cladocera *Bosmina* (*Bosmina*) *longirostris* and *Leptodora kindtii* (Fig. 5; Bjerring *et al.* 2009; Brancelj *et al.* 2009). Furthermore, taxa common in cold northern lakes, like *Paralona pigra*, *Alonopsis elongata*, *Rhynchotalona falcata* and *Eurycercus* spp., are or become absent (Nevalainen *et al.* 2013). This, together with the overall lowest species diversity in the sediment succession, confirms the persistence of rather exceptional environmental conditions, which are suitable only for specialized taxa (Goulden 1964; Hofmann 1978; Korhola & Rautio 2001).

Chronology

The Bayesian age-depth model for the core composite Co1410 is based on radiocarbon dates as well as tie points from the undisturbed sediment surface, ^{137}Cs and mercury data, and the pollen stratigraphy (Table 1; Fig. 8).

For the age-depth calculation, glacifluvial Unit I has been treated as an event layer (Fig. 8), because we assume a very rapid deposition in a fluvial system during deglaciation. Accordingly, the presumed grain-flow deposit incised into the glaciolacustrine Unit II (Subunit IIb) was treated as an event layer, originating in a mass movement. The age-depth model for the remainder of Unit II is based on pollen-derived ages of the Bølling/Allerød and Younger Dryas chronozones (Fig. 5), which refer to the chronozone boundary dated in northern Europe by Lohne *et al.* (2013) to 12 710±52 cal. a BP. The ages suggest, first, that the grain-flow deposition was associated with only little if any erosion, since the base of the Bølling/Allerød interstadial is clearly preserved in the lower part of Unit II. Second, the ages indicate that the radiocarbon dates obtained from Unit II are clearly too old, being biased by old organic carbon supplied from the catchment during deglaciation (Abbott & Stafford 1996; Björck *et al.* 2001). The decreasing offset of pollen and radiocarbon-derived ages towards the top of the unit probably reflects a reduced admixture of old organic carbon in the very low-productive lake during this period.

The sedimentation rates derived from the age-depth model show distinct variations. During the formation of the glaciolacustrine deposits of Unit II, sedimentation rates varied between 1.8 and 3.0 mm a^{-1} (Fig. 8). For the lacustrine deposits of Unit III the model shows much lower sedimentation rates between 0.5 and 0.9 mm a^{-1} and relatively constant sedimentation, probably because of the deduced retreat or absence of glaciers in the catchment. The rapid and strong increase in sedimentation rates of Unit IV to values between 5.4 and 5.6 mm a^{-1} indicates a distinct shift in the environmental conditions.

Climatic and environmental history

Lateglacial (>13 200–c. 11 550 cal. a BP)

The glacifluvial and glaciolacustrine deposits of Units I and II in core Co1410 (Figs 3–7) were formed during the Lateglacial between >13 200 and 11 550 cal. a BP (Fig. 8). According to the age-depth model, Unit I (Fig. 9A) and Subunit IIa (Fig. 9B) are attributed to the Bølling/Allerød chronozone, when relatively warm climate prevailed (Björck *et al.* 1998). In contrast, Subunits IIb, IIc and IId (Fig. 9C) are associated with the Younger Dryas chronozone, when relatively cool climatic conditions are reported (Lohne *et al.* 2013). According to the chronostratigraphical data derived from the pollen in core Co1410, the last ice-sheet coverage of the Imandra basin has to pre-date 13 200 cal. a BP. This is in good agreement with large-scale ice-sheet reconstructions for the LGM, which indicate that the SIS had inundated the Imandra region and reached its maximum extent around 20–18 cal. ka BP several hundred kilometres further to the east (Svendsen *et al.* 2004; Demidov *et al.* 2006; Hughes *et al.* 2016).

Moraines occurring in the vicinity of Lake Imandra are, however, mainly attributed to a local mountain glaciation in the Khibiny Mountains rather than to the SIS (Kolka & Korsakova 2005; Hättestrand *et al.* 2008; Kolka *et al.* 2008; Yevzerov & Nikolaeva 2008), and a few exposure ages derived recently by cosmogenic nuclide dating show a wide range between 16 and 11 ka BP (Stroeven *et al.* 2016). Partly ice-free conditions in the region already in the Bølling/Allerød chronozone are also indicated by studies of ice sheets and mountain glaciations in the Khibiny Mountains to the southeast of the coring location (Yevzerov & Nikolaeva 2008). The lake sediment cores hitherto retrieved in the region do not reach back to the time of initial deglaciation (Solovieva & Jones 2002; Solovieva *et al.* 2005; Olyunina *et al.* 2008; Ilyashuk *et al.* 2013; Tolstobrova *et al.* 2016; Shilova *et al.* 2019). As a consequence, reconstructions of the ice coverage in the Imandra region were for a

Table 1. Tie points and radiocarbon data obtained from Co1410 (OMR = organic macro-remain; T = twig; ST = small twig).

Sample ID	Composite depth (m)	Type	Fm	C (μg)	$\delta^{13}C$ (‰)	^{14}C age (a BP)	Calendar age (cal. a BP)	Error (a)
Surface	0						−68	1
Co1410_26-28	0.27	^{137}Cs					−36	10
Co1410_40-42	0.41	Hg					50	10
COL5648.1.0.0.1	1.04–1.06	Radiocarbon (OMR)	0.840±0.008	27		1398±81	1299	122
COL5649.1.0.0.1	3.32–3.34	Radiocarbon (OMR)	0.522±0.006	28		5227±92	6033	180
COL5650.1.0.0.1	4.12–4.14	Radiocarbon (ST)	0.414±0.004	31		7080±86	7787	160
COL5291.1.1	4.48–4.50	Radiocarbon (T)	0.369±0.002	997	−33.7	8017±51	9023	322
COL5652.1.0.0.1	5.04–5.06	Radiocarbon (T)	0.296±0.003	31		9769±92	11 231	166
COL5651.1.0.0.1	5.10–5.12	Radiocarbon (OMR)	0.287±0.003	36		10 032±93	11 540	291
Co1410_516-518	5.17	Pollen					11 700	100
Co1410_628-630	6.29	Pollen					12 300	100
COL5417.1.1	6.38–6.50	Radiocarbon (OMR)	0.203±0.006	147	1.3	12 792±231	15 105	830
COL5418.1.1	6.82–6.92	Radiocarbon (OMR)	0.122±0.005	156	−10.4	16 869±360	20 434	917
Co1410_768-770	7.79	Pollen					13 000	100
COL5419.1.1	7.78–7.86	Radiocarbon (OMR)	0.106±0.005	272	−5.4	18 003±374	21 733	910

long time based on large-scale interpolations, which indicated a deglaciation during the Younger Dryas chronozone (Lundqvist & Saarnisto 1995; Kleman *et al.* 1997; Boulton 2001; Svendsen *et al.* 2004; Hughes *et al.* 2016).

The time frame for the deglaciation proposed by these studies partly agrees with the results from core Co1410 from Lake Imandra. The initial, relatively early ice retreat is supported by the Rugozero and Kalevala moraines in the Karelian region and their equivalents at the northern coast of Kola Peninsula, which reflect the retreat of the SIS (Ekman *et al.* 1991; Rainio *et al.* 1995). The onset of continuous sediment accumulation in these regions, which suggests prevailing ice-free conditions, is dated to 14–13 cal. ka BP (Snyder *et al.* 1997, 2000; Kremenetski *et al.* 2004; Korsakova *et al.* 2016). This provides information about the timing of deglaciation of the Imandra region and thus suggests that the history reflected by core Co1410 starts only a few centuries after deglaciation of the site.

The depositional setting of the initial sediments of Unit I at coring site Co1410 most likely can be described as a braided river system, which was embedded within one of the larger, north–south orientated meltwater channels that developed in the Imandra region during the Lateglacial (Kleman *et al.* 1997; Hättestrand & Clark 2006a, b). These channels are up to several hundred metres wide and between a few decimetres and several metres deep (Kolka & Korsakova 2005; Kolka *et al.* 2008). The spillway is cut perpendicular to the flow direction in the west–east bounding hydro-acoustic profile (Fig. 3). There, the relief of the braided river at the end of the glacifluvial deposition may be reflected by the irregular shape of the blue reflector at the top of Unit I. This irregularity might be attributed to short-term and small-scale changes in braided river deposition (Williams & Rust 1969; Bridge *et al.* 2009), and is the reason for the different transitions between sediments of Unit I and Unit II (Fig. 6), whereof gradual transitions are attributed to riverbeds and abrupt changes to riverbanks.

Still during Bølling/Allerød times, glacifluvial sedimentation at coring site Co1410 passed over to glaciolacustrine sedimentation in a proglacial lake (Figs 8, 9). Pollen assemblages suggest a sparse vegetation cover and rather mild climate (Fig. 10), which is also documented further northward in coastal areas (Snyder *et al.* 2000; Corner *et al.* 2001). During the Younger Dryas chronozone, climate cooling and decreasing precipitation led to a decrease in vegetation cover and a re-advance of the SIS in Lake Imandra's catchment, which is reflected in changes of pollen, grain size, and MS (9; 10). Similar developments were reconstructed for the Younger Dryas along nearly all ice-marginal positions around the SIS (Lundqvist & Saarnisto 1995; Rainio *et al.* 1995; Demidov *et al.* 2006; Mangerud *et al.* 2011; Putkinen *et al.* 2011). The grain-flow deposit incised into the glaciolacustrine sediments of core Co1410 (Subunit IIb; Figs 4, 7) may have resulted from a high sediment supply during deglaciation, as observed for sub-recent glacier-induced mass movement deposits in the northern part of the Khibiny Mountains (Shilova *et al.* 2019).

The deglaciation of the Kola Region during the Lateglacial was associated with a marine transgression. This is reflected in brackish or marine sediments, which frequently overlay glacial diamictons along the northern coast of the Kola Peninsula and in the White Sea area (Corner *et al.* 1999; Snyder *et al.* 2000; Grøsfjeld *et al.* 2006; Korsakova *et al.* 2016). Even less than 30 km southwest of site Co1410 diatom analyses suggest a marine ingression during Lateglacial times (Tolstobrova *et al.* 2016). However, there is no such evidence at coring site Co1410. The Lateglacial sediment at this site lacks

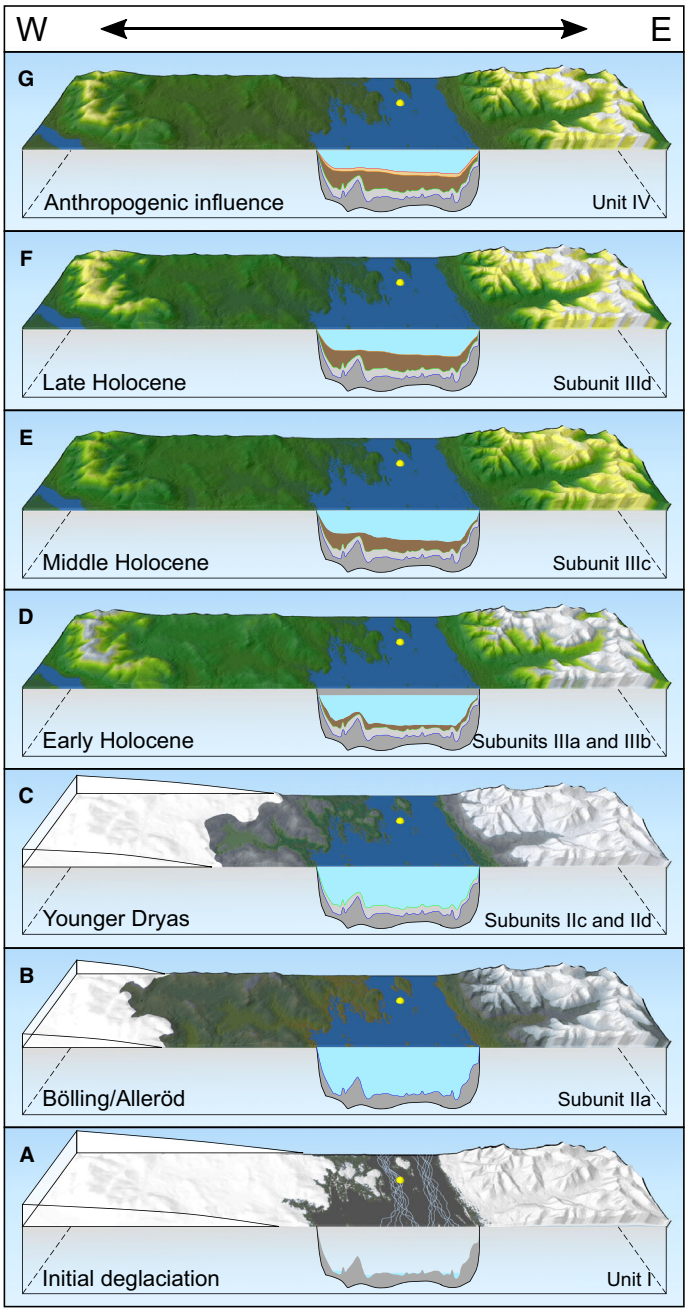

Fig. 9. W–E trending schematic block diagrams illustrating the environmental history in the vicinity of the coring site Co1410 (yellow circle). White colour indicates the SIS and local mountain glaciation in the west and east, respectively. Lake bathymetry and sediment architecture are derived from the seismic profile presented in Fig. 3 and suggest the different stages of sediment deposition. A and B = Ice retreat and transition from glacifluvial sedimentation in a braided river setting to glaciolacustrine sedimentation in a proglacial lake during the Bølling/Allerød interstadial; C = glacial re-advances during the Younger Dryas chronozone; D = retreat of the SIS from the palaeocatchment area until the beginning of the Early Holocene under the presence of mountain glaciers and establishment of forests around the lake; E = completely ice-free conditions in the catchment during the Middle Holocene and migration of the tree line to high altitudes; F = build-up of small mountain glaciers in the Late Holocene and migration of the tree line downward; G = retreat of the mountain glaciers nowadays and sediment deposition under the influence of anthropogenic activities in the catchment area. The block diagrams are based on ASTER Global Digital Elevation Model (GDEM) Version 3 (NASA/METI/AIST/Japan Spacesystems 2001), including ASTER Global Water Bodies Database (ASTWBD) Version 1 (NASA/METI/AIST/Japan Spacesystems 2019) to correct elevation values of water body surfaces.

marine shell fragments, and very low S contents (Fig. 4) clearly argue against brackish or marine conditions (Berner & Raiswell 1984).

Early Holocene (c. 11 550–8400 cal. a BP)

The change from glaciolacustrine to lacustrine conditions in Lake Imandra is reflected by the onset of Unit III deposition (Figs 4, 5), which is dated to *c.* 11 550 cal. a BP (Fig. 8) and about 100 years delayed compared to supra-regional records (Stroeven *et al.* 2016) as well as the NGRIP ice-core record (Walker *et al.* 2009; Rasmussen *et al.* 2014). However, this age is in good accordance with regional records to the west of Lake Imandra and at the northern coast of Kola Peninsula, which show the same characteristics (Snyder *et al.* 2000; Solovieva & Jones 2002; Kremenetski *et al.* 2004), and coincides very well with the Younger Dryas to Holocene boundary in northern Europe, which was dated by Lohne *et al.* (2013) to 11 549±59 cal. a BP.

The period until 8400 cal. a BP, comprising deposition of Subunits IIIa and IIIb in core Co1410, is assigned to the Early Holocene (Figs 8, 9). Physical properties and geochemical data in this part of the record reflect that the Lateglacial to Early Holocene transition was associated with a strong reduction of glacial influence on sedimen-

tation, suggesting that the ice mass mainly responsible for this, the SIS, had retracted from the lake's catchment and mountain glaciers are strongly reduced in size (Figs 4, 9, 10). However, the latter may have persisted, as indicated by a delayed onset of full lacustrine conditions in small lakes in the Khibiny Mountains (Olyunina *et al.* 2008; Shilova *et al.* 2019). Changes in the cladoceran assemblages in core Co1410 are characteristic of the transitions from glacial to postglacial conditions (Korhola *et al.* 2001; Bledzki & Rybak 2016). Furthermore, they suggest that the lake level of Lake Imandra at the onset of the Early Holocene was low (Fig. 10), coincident with lake-level drops in other large basins on the Kola Peninsula (Shvarev 2003; Olyunina *et al.* 2008).

Pollen data of core Co1410 suggest that rather sparsely covered landscapes were successively replaced by denser vegetation in a warming and moister climate during the course of the Early Holocene (Fig. 10). This change is also recorded in other areas of northwestern Russia (Snyder *et al.* 2000; Arslanov *et al.* 2001; Wohlfarth *et al.* 2004; Ilyashuk *et al.* 2013; Nikolaeva *et al.* 2015), and matches with a pronounced shift to higher surface temperatures in the Norwegian Sea around 9300 a BP (Koç *et al.* 1993), when moist and warm North Atlantic air masses replaced high Arctic air masses (Hammarlund *et al.* 2002; Jones *et al.* 2004).

In Subunit IIIa (Fig. 8; 11 550–8850 cal. a BP; Fig.) more short-term climate variations are indicated by some of the high-resolution biogeochemical data. Peaks in proxies reflecting lithogenic supply (e.g. Ti/Al, K/Al, Zr/Al; Figs 4, 10) are probably attributed to cooling events, such as those recorded in a number of North Atlantic marine, terrestrial and ice-core records at 11 400, 10 400–10 300 and *c.* 9400 cal. a BP (Björck *et al.* 1997, 2001; Bond *et al.* 1997; Nesje *et al.* 2001; Yu & Wright 2001; Rasmussen *et al.* 2014). These climatic variations may also have led to unstable redox conditions in Lake Imandra, as suggested by short-term variability in redox-sensitive geochemical proxies (e.g. Fe/Mn; Fig. 10). Such changes, although detected with limited age control, were also determined in other studies in the Kola region and attributed to a transitional phase towards more stable lacustrine conditions (Snyder *et al.* 1997; Corner *et al.* 1999, 2001).

In Subunit IIIb (Fig. 8; 8850–8400 cal. a BP) the sedimentological and palynological proxies (e.g. TI/Al, Si/Ti, TOC, grain size, *Pinus*; Fig. 10) indicate cooler climatic conditions. A potential correlation of this cooling with the 8.2 ka cooling event (Alley *et al.* 1997; Magny *et al.* 2003; Rohling & Pälike 2005) would imply a dating uncertainty in the order of several hundred years in this part of the record. The 8.2 ka event was identified in a sediment record to the east of Lake Imandra by a chironomid-based temperature reconstruction (Fig. 10; Ilyashuk *et al.* 2013), but is not documented in the multi-proxy study on a lake sediment core to the west (Jones *et al.* 2004). The latter supports the interpretation of a decreasing significance of Atlantic climatic signals from Norwegian coastal areas to the central Kola region, which was deduced from pollen records (Korhola *et al.* 2004; Solovieva *et al.* 2005; and Seppä *et al.* 2007).

Middle and Late Holocene (8400–30 cal. a BP)

The lacustrine Subunits IIIc and IIId in core Co1410 were deposited in the periods 8400–3700 and 3700–30 cal. a BP (Fig. 8), which are assigned to the Middle and Late Holocene, respectively.

The Middle Holocene was, according to the pollen and cladoceran data of core Co1410 (Figs 5, 10), characterized by a particularly warm climate, which led to a dense vegetation in the catchment of Lake Imandra and probably the disappearance of glaciers in the adjacent Khibiny Mountains (Fig. 9E). The Holocene Thermal Maximum (HTM) recorded between 8000 and 4600 cal. a BP at Lake Imandra is slightly delayed compared to other reconstructions of the HTM in the central Kola region, which are based on micropalaeontological analyses that confine this period to 9000–5000 cal. a BP (Solovieva & Jones 2002; Kremenetski *et al.* 2004; Ilyashuk *et al.* 2013). However, it is within the overall range of HTM reconstructions in northwestern Europe, for instance in southern Finland from 7500–4000 cal. a BP (Ojala *et al.* 2008), in the northeastern European Russian Arctic from 8000 to 3500 cal. a BP (Salonen *et al.* 2011), in Latvia from 8000 to 4500 cal. a BP (Heikkila & Seppä 2010) and in north Sweden from 9500 to 3400 cal. a BP (Meyer-Jacob *et al.* 2017). The differences in the timing of the HTM could be a result of supra-regional shifts; however, the lack of obvious spatial trends rather suggests inaccuracies in the climate reconstructions and chronological uncertainties.

Rather small variations in almost all physical and geochemical proxies in the Middle Holocene deposits of core Co1410 (Figs 4, 10), compared to the Early Holocene, suggest prevailing stable climatic conditions. This supports the suggestion that the climate in Fennoscandia during the HTM was controlled by a higher insolation and rather stable anti-cyclonic conditions during summer as compared to today (Seppä & Birks 2001; Bakke *et al.* 2005; St. Amour *et al.* 2010).

For the Late Holocene, the proxies of core Co1410 suggest a slight cooling, with a somewhat reduced vegetation cover, increased input of lithogenic material, including aeolian supply, and an increase in aquatic production. The cooling may have been associated with an increase in humidity, as indicated by the development of widespread wetlands in the area simultaneous with retreating forests (Hammarlund *et al.* 2004; Weckstrom *et al.* 2010; Valiranta *et al.* 2011). Micropalaeontological investigations of lake archives in the vicinity of Lake Imandra also document wetter conditions during this period (Jones *et al.* 2004; Solovieva *et al.* 2005; Ilyashuk

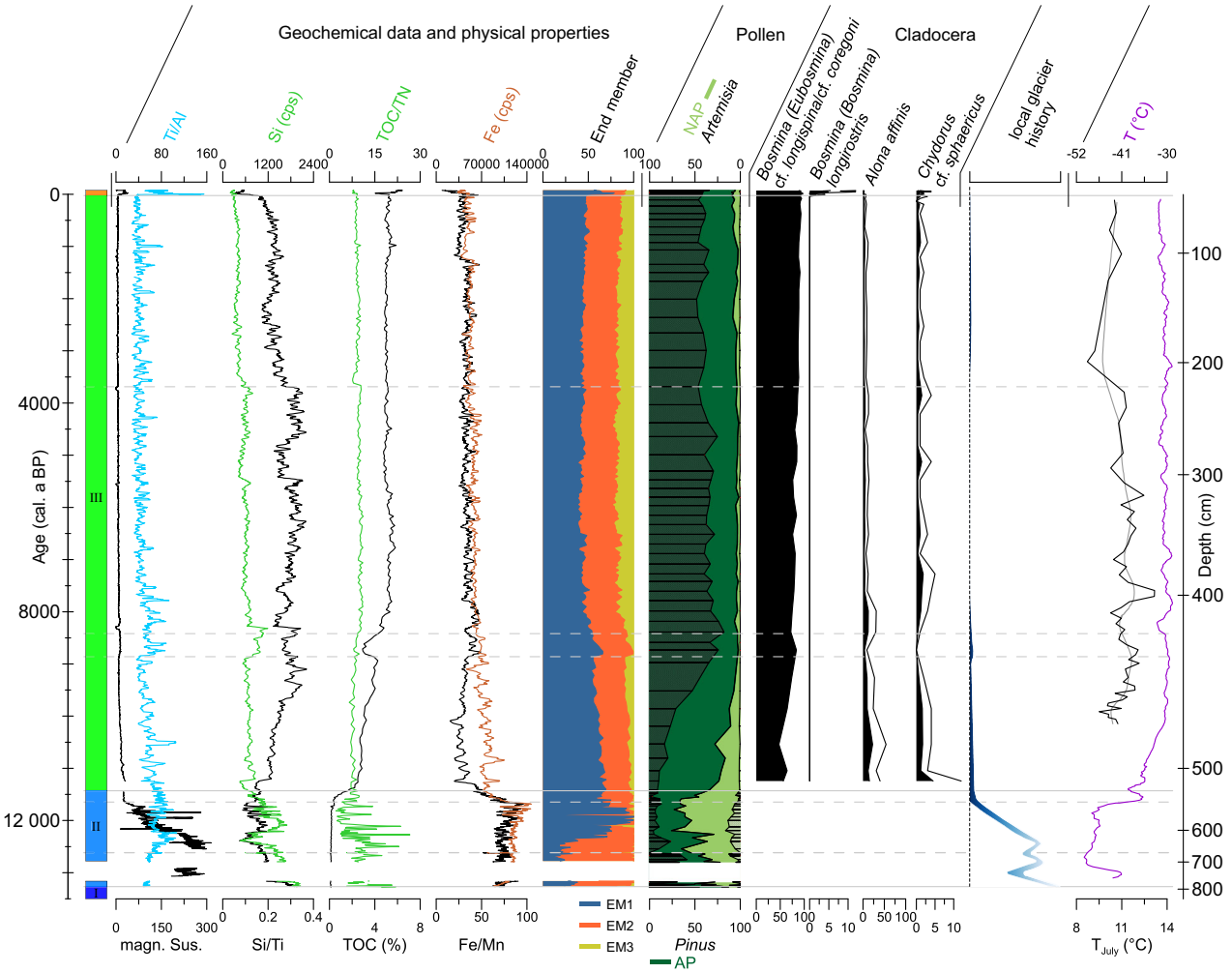

Fig. 10. Sedimentary units and selected physical property, geochemical, pollen, and cladoceran data from core Co1410 plotted against calibrated age (*y*-axis). Note that pollen, cladoceran and end-member calculations are presented in % and partly share one *x*-axis. The data are compared to the local Scandinavian Ice Sheet (SIS) and mountain glacier histories reconstructed here (bluish shadings) as well as the local July temperature from Ilyashuk *et al.* (2013), the LOESS-smoothed record (span = 0.20, order = 1; grey line), and the δ^{18}O-derived annual temperature from the GISP2 ice-core (Cuffey & Clow 1997; Alley 2000) using the calibration from Cuffey *et al.* (1995) (violet line).

et al. 2013; Nikolaeva *et al.* 2015). Both the cooling and the increased humidity may have their origin in a weakening of the prevailing anti-cyclonic circulation patterns (Seppä & Birks 2001, 2002; Wanner *et al.* 2008), and may have supported the reactivation of local mountain glaciers in the vicinity of the lake, such as those occurring today in the Khibiny Mountains (Fig. 9; Demin & Zyuzin 2006; Khromova *et al.* 2014). A reoccurrence of glaciers was also reconstructed for the Late Holocene in northern Sweden (Snowball & Sandgren 1996; Nesje *et al.* 2001).

Anthropogenic influence (since 30 cal. a BP)

The lacustrine deposits of Unit IV in core Co1410 reflect the human impact on Lake Imandra's catchment during the past *c.* 100 years.

Subunit IVa reflects enhanced input of lithogenic material of particularly fine-grained particles along with an increase in aeolian sediment supply and a change in cladoceran assemblages (Fig. 10). These changes can be traced back to human impact in the course of an intensification of land use since the end of the 19th century, and especially to industrial and mining activities in the catchment area as well as direct wastewater dumping into the lake since the early AD 1920s (Dauvalter *et al.* 1999b; Moiseenko *et al.* 2002, 2009b; Rigina 2002; Voinov *et al.* 2004). Enhanced sediment supply is obvious from studying aerial photographs taken in the AD 1960s that show the distribution of a sediment fan in Bolshaya Imandra originating from the mouth of Belaya River (Kravtsova 1995). Sediment deposits in the south-eastern part of Bolshaya Imandra, in the vicinity of the river mouth, exceed a thickness of 8 m (Chidzikov 1980).

The anthropogenically induced modifications of the lake water characteristics are also evident in various studies on fishes and smaller organisms (Chidzikov 1980; Moiseenko *et al.* 2002, 2009a; Lukin 2013).

The transition from Subunits IVa to IVb reflects the reduction of fine-grained lithogenic sediment input and aeolian supply. The level of pollution and trophic state is also reduced but remains elevated compared to the natural state. These changes are associated with enhanced environmental protection and reduced industrial production (Fig. 7; Voinov *et al.* 2004), as well as the build-up of a dam in the AD 1960s, which according to aerial photographs has efficiently reduced industrially induced sediment input (Rigina 2002). Besides shifts in the anthropogenic impact, pollen spectra in core Co1410 (Fig. 10) indicate a warmer and drier climate that is also recorded since the AD 1950s by long-term meteorological observations (Demin & Zyuzin 2006; Marshall *et al.* 2016), and an upward shift of the tree line of around 100 m in the Khibiny Mountains (Fig. 9; Demin & Zyuzin 2007; Mathisen *et al.* 2014), as well as changes in the growing seasons in Lake Imandra's catchment (Karlsen *et al.* 2006; Høgda *et al.* 2013).

Conclusions

Hydro-acoustic data and different proxies from an 8.46-m-long sediment succession with a basal age of 13 200 cal. a BP from Lake Imandra allow us to draw the following conclusions concerning the regional environmental and climatic history:

- The hydro-acoustic data show the existence of large channels, which can be attributed to meltwater channels that formed large glacifluvial systems during the initial deglaciation of the area prior to 13 200 cal. a BP. According to the sediment core data, glaciolacustrine deposits filled these channels successively until *c.* 11 550 cal. a BP and drape the bottom morphology. Subsequently, lacustrine sediments levelled the underlying topography until recent times.
- Pollen assemblages indicate the initial deglaciation during the Bølling/Allerød chronozone. At least one glacial advance is documented during the Younger Dryas chronozone. Another, smaller advance of glaciers in the Khibiny Mountains in the Early Holocene is indicated in the physical properties of grain size and MS, as well as the geochemical proxies Rb/Sr and Zr/Rb. They reflect changing energetic levels in the lake basin in dependence on the proximity of the ice margin or the existence of small ice caps in the mountain regions.
- With the onset of the Holocene at *c.* 11 550 cal. a BP, greyish glaciolacustrine sediment deposition changed to brownish lacustrine sedimentation and the pollen assemblages indicate a shift from cold glacial to warmer interglacial temperatures. Increasing diversity of the cladoceran assemblages and higher amounts of TOC can be attributed to a higher productivity in the lake and its catchment, respectively.
- A short-term cold event can be reconstructed from a decrease of TOC and Si/Ti between 8800 and 8400 cal. a BP, which can be attributed to the 8.2 ka cooling event within the limits of our age-depth model. The Holocene Thermal Maximum (HTM) is recorded between 8000 and 4600 cal. a BP and indicated by the highest concentration of *Pinus* pollen and highest AP/NAP ratios of the sediment succession. During the later Holocene between 4600 and 30 cal. a BP, a slight cooling and increased aeolian activity is documented in a decrease of *Pinus* pollen and higher Zr/Al ratios, respectively.
- During the last century, the dramatic influence of industrial activity in the catchment area is documented in a sharp lithological shift. A rapidly increasing sediment supply is a consequence of mining activities and wastewater dumping. Biogeochemical proxies and cladoceran assemblages indicate high levels of pollution and eutrophication of the water column.
- Our results show that biogeochemical and micropaleontological-based climatic and environmental history reconstruction agrees well with other studies from the Kola Peninsula highlighting vegetation and climatic changes in this area. Moreover, the record from core Co1410 specifies the deglaciation pattern for the central Kola Peninsula, which previously was based on wide interpolations and only a few dates. Within the uncertainty of the age model, the Holocene palaeoenvironmental history recorded in Lake Imandra is in general agreement with observations made in nearby Lakes Chuna and Kupal'noe. However, all lakes react slightly differently to climatic events and seem to be influenced by local effects. Size and geographical position should be taken into consideration when studying lake archives and comparing them with each other.

Acknowledgements. – Financial support for this study was provided by the German Research Foundation (DFG – grant no. ME 1169/28), St. Petersburg State University (SPBU – grant no. 18.65.39.2017) and the German Federal Ministry of Education and Research (BMBF – grant no. 03G0859A). The work of G. Fedorov and N. Kostromina was also sponsored by the Russian Foundation for Basic Research (grant 18-05-60291). L. Frolova was supported by the Russian Government Program of Competitive Growth of Kazan Federal University and by a grant from the Russian Scientific Foundation (project 20-17-00135). We are grateful to various colleagues from the Geological Institute of the Kola Science Centre of Russian Academy of Sciences (GI KSC RAS) in Apatity for their expertise and logistical help during the fieldwork in summer 2017. We thank Nicole Mantke and Dorothea Klinghardt from the University of Cologne for assistance and help with the laboratory work. We also thank the two anonymous reviewers as well as editor Jan A. Piotrowski for their constructive comments. The authors declare no conflict of interest. All data are accessible in the Pangaea data repository.

Author contributions. – ML, GF, VK, BW and MMe designed the study ML, LS, LF, AC, MMo, NK and NN performed the analyses. ML wrote the paper and prepared the figures with input from all co-authors.

References

Abbott, M. B. & Stafford, T. W. 1996: Radiocarbon geochemistry of modern and ancient Arctic lake systems, Baffin Island, Canada. *Quaternary Research 45*, 300–311.

Alley, R. B. 2000: Ice-core evidence of abrupt climate changes. *Proceedings of the National Academy of Sciences 97*, 1331–1334.

Alley, R. B., Mayewski, P. A., Sowers, T., Stuiver, M., Taylor, K. C. & Clark, P. U. 1997: Holocene climatic instability: a prominent, widespread event 8200 yr ago. *Geology 25*, 483–486.

Armand, N. N., Evzerov, V. Y., Gunova, V. S. & Lebedeva, P. M. 1969: Paleogeografiya tsenral'noi chasti Kol'skogo poluostrova v golotsene. *In* Grave, M. K. & Koshechkin, B. I. (eds.): *Osnovnye Problemy Geomorfologii i Stratigrafii Antropogena Kol'skogo Poluostrova*, 80–85. Nauka, Leningrad.

Arslanov, K. A., Savelieva, L. A., Klimanov, V. A., Chernov, S. B., Maksimov, F. E., Tertychnaya, T. V. & Subetto, D. A. 2001: New data on chronology of landscape-paleoclimatic stages in northwestern Russia during the Late Glacial and Holocene. *Radiocarbon 43*, 581–594.

Bakke, J., Dahl, S. O., Paasche, O., Løvlie, R. & Nesje, A. 2005: Glacier fluctuations, equilibrium-line altitudes and palaeoclimate in Lyngen, northern Norway, during the Lateglacial and Holocene. *Holocene 15*, 518–540.

Beck, P. S. A., Jönsson, P., Høgda, K. A., Karlsen, S. R., Eklundh, L. & Skidmore, A. K. 2007: A ground-validated NDVI dataset for monitoring vegetation dynamics and mapping phenology in Fennoscandia and the Kola peninsula. *International Journal of Remote Sensing 28*, 4311–4330.

Beckhoff, B., Kanngießer, B., Langhoff, N., Wedell, R. & Wolff, H. 2006: *Handbook of Practical X-Ray Fluorescence Analysis*. 848 pp. Springer, Berlin.

Berglund, B. E. & Ralska-Jasiewiczowa, M. 1986: Pollen analysis and pollen diagrams. *In* Berglund, B. (ed.): *Handbook of Holocene Palaeoecology and Palaeohydrology*, 455–484. Wiley Interscience, New York.

Berner, R. A. & Raiswell, R. 1984: C/S method for distinguishing freshwater from marine sedimentary rocks. *Geology 12*, 365–368.

Bertin, E. P. 1975: *Principles and Practice of X-Ray Spectrometric Analysis*. 945 pp. Springer US, Boston.

Bjerring, R., Becares, E., Declerck, S., Gross, E. M., Hansson, L. A., Kairesalo, T., Nykänen, M., Halkiewicz, A., Kornijów, R., Conde-Porcuna, J. M., Seferlis, M., Nöges, T., Moss, B., Amsinck, S. L., Odgaard, B. V. & Jeppesen, E. 2009: Subfossil Cladocera in relation to contemporary environmental variables in 54 Pan-European lakes. *Freshwater Biology 54*, 2401–2417.

Björck, S., Muscheler, R., Kromer, B., Andresen, C. S., Heinemeier, J., Johnsen, S. J., Conley, D., Koç, N., Spurk, M. & Veski, S. 2001: High-resolution analyses of an early Holocene climate event may imply decreased solar forcing as an important climate trigger. *Geology 29*, 1107–1110.

Björck, S. & Wohlfarth, B. 2001: ^{14}C Chronostratigraphic techniques in paleolimnology. *In* Last, W. M. & Smol, J. P. (eds.): *Tracking Environmental Change Using Lake Sediments*, 205–245. Springer Netherlands, Dordrecht.

Björck, S., Rundgren, M., Ingólfsson, Ó. & Funder, S. 1997: The Preboreal oscillation around the Nordic Seas: terrestrial and lacustrine responses. *Journal of Quaternary Science 12*, 455–465.

Björck, S., Walker, M. J. C., Cwynar, L. C., Johnsen, S., Knudsen, K. L., Lowe, J. J. & Wohlfarth, B. 1998: An event stratigraphy for the Last Termination in the north Atlantic region based on the Greenland ice-core record: a proposal by the INTIMATE group. *Journal of Quaternary Science 13*, 283–292.

Blaauw, M. & Christen, J. A. 2011: Flexible paleoclimate age-depth models using an autoregressive gamma process. *Bayesian Analysis 6*, 457–474.

Blaauw, M., Christen, J. A., Vazquez, J. E., Belding, T., Theiler, J., Gough, B. & Karney, C. 2020: Package 'rbacon' - Age-Depth Modelling using Bayesian Statistics. Queen's University Belfast, 55 pp.

Bledzki, L. A. & Rybak, J. I. 2016: *Freshwater Crustacean Zooplankton of Europe. Cladocera & Copepoda (Calanoida, Cyclopoida) Key to Species Identification, with Notes on Ecology, Distribution, Methods and Introduction to Data Analysis*. 918 pp. Springer International Publishing, Cham.

Blott, S. J. & Pye, K. 2001: GRADISTAT: a grain size distribution and statistics package for the analysis of unconsolidated sediments. *Earth Surface Processes and Landforms 26*, 1237–1248.

Bond, G., Showers, W., Cheseby, M., Lotti, R., Almasi, P., deMenocal, P., Priore, P., Cullen, H., Hajdas, I. & Bonani, G. 1997: A pervasive millennial-scale cycle in North Atlantic Holocene and glacial climates. *Science 278*, 1257–1266.

Boulton, G. 2001: Palaeoglaciology of an ice sheet through a glacial cycle: the European ice sheet through the Weichselian. *Quaternary Science Reviews 20*, 591–625.

Brancelj, A., Kernan, M., Jeppesen, E., Rautio, M., Manca, M., Sisko, M., Alonso, M. & Stuchlik, E. 2009: Cladocera remains from the sediments of remote cold lakes: a study of 294 lakes across Europe. *Advances in Limnology 62*, 269–294.

Bridge, J. S. & Lunt, I. A. 2009: Depositional models of braided rivers. *In* Jarvis, I., Sambrook Smith, G. H., Best, J. L., Bristow, C. S. & Petts, G. E. (eds.): *Braided Rivers*, 11–50. Wiley-Blackwell, Malden.

Bro, R. & Smilde, A. K. 2014: Principal component analysis. *Analytical Methods 6*, 2812–2831.

Brown, E. T., Johnson, T. C., Scholz, C. A., Cohen, A. S. & King, J. W. 2007: Abrupt change in tropical African climate linked to the bipolar seesaw over the past 55,000 years. *Geophysical Research Letters 34*, L20702. https://doi.org/10.1029/2007GL031240.

Bryant, C. L., Farmer, J. G., MacKenzie, A. B., Bailey-Watts, A. E. & Kirika, A. 1997: Manganese behavior in the sediments of diverse Scottish freshwater lochs. *Limnology and Oceanography 42*, 918–929.

Chidzikov, V. V. 1980: Hydro-chemistry and bottom sediments of the Imandra Lake under impact of industrial pollution. *The Ecosystem of the Imandra Lake under Impact of Industrial Pollution* Kola Science Centre, Apatity, 24–64. (in Russian).

Cohen, A. S. 2003: *Paleolimnology: the History and Evolution of Lake Systems*. 528 pp. Oxford University Press, New York.

Corner, G. D., Kolka, V. V., Yevzerov, V. Y. & Møller, J. J. 2001: Postglacial relative sea-level change and stratigraphy of raised coastal basins on Kola Peninsula, northwest Russia. *Global and Planetary Change 31*, 155–177.

Corner, G. D., Yevzerov, V. Y., Kolka, V. V. & Møller, J. J. 1999: Isolation basin stratigraphy and Holocene relative sea-level change at the Norwegian-Russian border north of Nikel, northwest Russia. *Boreas 28*, 146–166.

Croudace, I. W., Rindby, A. & Rothwell, R. G. 2006: ITRAX: description and evaluation of a new multi-function X-ray core scanner. *Geological Society, London, Special Publications 267*, 51–63.

Cuffey, K. M. & Clow, G. D. 1997: Temperature, accumulation, and ice sheet elevation in central Greenland through the last deglacial transition. *Journal of Geophysical Research: Oceans 102*, 26383–26396.

Cuffey, K. M., Clow, G. D., Alley, R. B., Stuiver, M., Waddington, E. D. & Saltus, R. W. 1995: Large Arctic temperature change at the Wisconsin-Holocene Glacial Transition. *Science 270*, 455–458.

Cuven, S., Francus, P. & Lamoureux, S. 2011: Mid to Late Holocene hydroclimatic and geochemical records from the varved sediments of East Lake, Cape Bounty, Canadian High Arctic. *Quaternary Science Reviews 30*, 2651–2665.

Dauvalter, V. A. & Kashulin, N. A. 2015: Changes in concentrations of nickel and copper in the surface layers of sediments of the Lake Imandra the last half century. *Vestnik MGTU 18*, 307–321.

Dauvalter, V. A. & Kashulin, N. A. 2018: Mercury pollution of Lake Imandra sediments, the Murmansk region, Russia. *International Journal of Environmental Research 12*, 939–953.

Dauvalter, V., Moiseenko, T. I. & Rodyushkin, I. V. 1999a: Geochemistry of rare earth elements in Imandra Lake, Murmansk area. *Geochemistry International 37*, 325–331.

Dauvalter, V., Moiseenko, T. I., Rodyushkin, I. V., Kudryavtseva, L. P. & Sharov, A. N. 1999b: Sulfur migration and cycle in a subarctic lake contaminated by wastes of a mining complex: a case study of Lake Imandra. *Geochemistry International 37*, 552–561.

Davies, S. J., Lamb, H. F. & Roberts, S. J. 2015: Micro-XRF core scanning in palaeolimnology: recent developments. *In* Croudace, I. W. & Rothwell, R. G. (eds.): *Micro-XRF Studies of Sediment Cores*, 189–226. Springer Netherlands, Dordrecht.

Davydova, N. & Servant-Vildary, S. 1996: Late Pleistocene and Holocene history of the lakes in the Kola Peninsula, Karelia and the north-western part of the East European Plain. *Quaternary Science Reviews 15*, 997–1012.

Demidov, I. N., Houmark-Nielsen, M., Kjær, K. H. & Larsen, E. 2006: The last Scandinavian Ice Sheet in northwestern Russia: ice flow patterns and decay dynamics. *Boreas 35*, 425–443.

Demin, V. I. & Zyuzin, Y. L. 2006: On climatic changes in the Khibiny Mountains (Kola Peninsula, Russia). *Physics of Auroral Phenomena 24*, 281–284.

Demin, V. I. & Zyuzin, Y. L. 2007: Meteorological observations at the mountaintop stations in the Khibiny (the Kola Peninsula, Russia) and regional climatic changes. *International Conference on Alpine Meteorology*, p. 4.

Dewald, A., Heinze, S., Jolie, J., Zilges, A., Dunai, T., Rethemeyer, J., Melles, M., Staubwasser, M., Kuczewski, B., Richter, J., Radtke, U., von Blanckenburg, F. & Klein, M. 2013: CologneAMS, a dedicated center for accelerator mass spectrometry in Germany. *Nuclear Instruments & Methods in Physics Research Section B-Beam Interactions with Materials and Atoms 294*, 18–23.

Doncheva, A. V. & Kalutskov, V. N. 1977: Prediction of the environmental impact of mining and metallurgical production in the tayga zone (with reference to the copper-nickel complexes of Mochegorsk and Sudbury). *Soviet Geography 18*, 223–229.

Ekman, I. & Iljin, V. 1991: Deglaciation, the Younger Dryas end moraines and their correlation in the Karelian ASSR and adjacent areas. *In* Rainio, H. & Saarnisto, M. (eds.): *IGCP Project 253, Termination of the Pleistocene, Eastern Fennoscandian End Moraines, Field Conference North Karelia, Finland and Karelian ASSR, June 26–July 4, 1991*, 73–99. Geological Survey of Finland, Espoo.

Elshin, Y. A. & Kupriyanov, V. V. 1970: *Resources of the Surface Waters of the USSR, Vol. 1, Kola Peninsula*. 316 pp. Gidrometeoizdat, Leningrad (in Russian).

Elverhøi, A., Fjeldskaar, W., Solheim, A., Nyland-Berg, M. & Russwurm, L. 1993: The Barents Sea Ice Sheet — A model of its growth and decay during the last ice maximum. *Quaternary Science Reviews 12*, 863–873.

Engstrom, D. R. & Wright, H. E. J. 1984: *Chemical Stratigraphy of Lake Sediments as a Record of Environmental Change*. 230 pp. Leicester University Press, Leicester.

Favre, E., Escarguel, G., Suc, J. P., Vidal, G. & Thévenod, L. 2008: A contribution to deciphering the meaning of AP/NAP with respect to vegetation cover. *Review of Palaeobotany and Palynology 148*, 13–35.

Flößner, D. 2000: *Die Haplopoda und Cladocera (ohne Bosminidae) Mitteleuropas*. 428 pp. Backhuys, Leiden.

Folk, R. L. & Ward, W. C. 1957: Brazos River bar: a study in the significance of grain size parameters. *Journal of Sedimentary Research 27*, 3–26.

Frey, D. G. 1959: The taxonomic and phylogenetic significance of the head pores of the Chydoridae (Cladoceha). *International Review of Hydrobiology 44*, 27–50.

Frey, D. G. 1973: Comparative morphology and biology of three species of *Eurycercus* (Chydoridae, Cladocera) with a description of *Eurycercus macrocanthus* sp. nov. *Internationale Revue der gesamten Hydrobiologie und Hydrographie 58*, 221–267.

Gee, G. W. & Or, D. 2002: Particle-size analysis. In Dane, J. H., Topp, G. C. & Campbell, G. S. (eds.): *Methods of Soil Analysis, Part 4, Physical Methods*, 255–293. Soil Science Society of America, Madison.

Geotek 2016: *Multi-Sensor Core Logger*. 232 pp. GEOTEK Ltd, Northamptonshire.

Goulden, C. E. 1964: The history of the Cladoceran fauna of Esthwaite water (England) and its limnological significance. *Archives of Hydrobiology 60*, 1–52.

Gromig, R., Wagner, B., Wennrich, V., Fedorov, G., Savelieva, L., Lebas, E., Krastel, S., Brill, D., Andreev, A., Subetto, D. & Melles, M. 2019: Deglaciation history of Lake Ladoga (northwestern Russia) based on varved sediments. *Boreas 48*, 330–348.

Grøsfjeld, K., Funder, S., Seidenkrantz, M.-S. & Glaister, C. 2006: Last Interglacial marine environments in the White Sea region, northwestern Russia. *Boreas 35*, 493–520.

Håkanson, L. 1977: The influence of wind, fetch, and water depth on the distribution of sediments in Lake Vänern, Sweden. *Canadian Journal of Earth Sciences 14*, 397–412.

Hammarlund, D., Barnekow, L., Birks, H. J. B., Buchardt, B. & Edwards, T. W. D. 2002: Holocene changes in atmospheric circulation recorded in the oxygen-isotope stratigraphy of lacustrine carbonates from northern Sweden. *The Holocene 12*, 339–351.

Hammarlund, D., Velle, G., Wolfe, B. B., Edwards, T. W. D., Barnekow, L., Bergman, J., Holmgren, S., Lamme, S., Snowball, I., Wohlfarth, B. & Possnert, G. 2004: Palaeolimnological and sedimentary responses to Holocene forest retreat in the Scandes Mountains, west-central Sweden. *Holocene 14*, 862–876.

Hammer, Ø., Harper, D. A. T. & Ryan, P. D. 2001: PAST: paleontological statistics software package for education and data analysis. *Palaeontologia Electronica 4*, http://palaeo-electronica.org/2001_1/past/issue1_01.htm.

Hann, B. J. & Warner, B. G. 1987: Late Quaternary Cladocera from coastal British Columbia, Canada: A record of climatic or limnologic change? *Archives of Hydrobiology 110*, 161–177.

Harmsworth, R. V. 1968: The developmental history of Blelham Tarn (England) as shown by animal microfossils, with special reference to the Cladocera. *Ecological Monographs 38*, 223–241.

Hättestrand, C. & Clark, C. D. 2006a: The glacial geomorphology of Kola Peninsula and adjacent areas in Murmansk Region, Russia. *Journal of Maps 2*, 30–42.

Hättestrand, C. & Clark, C. D. 2006b: Reconstructing the pattern and style of deglaciation of Kola Peninsula, Northeastern Fennoscandian Ice Sheet. *In* Knight, P. (ed.): *Glacier Science and Environmental Change Glacier Science and Environmental Change*, 199–201. Blackwell Publications, Malden.

Hättestrand, C., Kolka, V. & Johansen, N. 2008: Cirque infills in the Khibiny mountains, Kola Peninsula, Russia - palaeoglaciological interpretations and modern analogues in East Antarctica. *Journal of Quaternary Science 23*, 165–174.

Heikkila, M. & Seppä, H. 2010: Holocene climate dynamics in Latvia, eastern Baltic region: a pollen-based summer temperature reconstruction and regional comparison. *Boreas 39*, 705–719.

Hennekam, R. & de Lange, G. 2012: X-ray fluorescence core scanning of wet marine sediments: methods to improve quality and reproducibility of high-resolution paleoenvironmental records. *Limnology and Oceanography-Methods 10*, 991–1003.

Herdendorf, C. E. 1982: Large lakes of the world. *Journal of Great Lakes Research 8*, 379–412.

Hofmann, W. 1978: *Bosmina (Eubosmina)* populations of Großer Pläner See and Schöhsee lakes during late-glacial and postglacial times. *Polish Archives of Hydrobiology 25*, 167–176.

Hofmann, W. 1987: Cladocera in space and time: analysis of lake sediments. *Hydrobiologia 145*, 315–321.

Hofmann, W. 1996: Empirical relationships between cladoceran fauna and trophic state in thirteen northern German lakes: analysis of surficial sediments. *Hydrobiologia 318*, 195–201.

Høgda, K., Tømmervik, H. & Karlsen, S. 2013: Trends in the start of the growing season in Fennoscandia 1982-2011. *Remote Sensing 5*, 4304–4318.

Hua, Q., Barbetti, M. & Rakowski, A. Z. 2013: Atmospheric radiocarbon for the period 1950-2010. *Radiocarbon 55*, 2059–2072.

Hughes, A. L. C., Gyllencreutz, R., Lohne, O. S., Mangerud, J. & Svendsen, J. I. 2016: The last Eurasian ice sheets - a chronological database and time-slice reconstruction, DATED-1. *Boreas 45*, 1–45.

Ilyashuk, E. A., Ilyashuk, B. P., Kolka, V. V. & Hammarlund, D. 2013: Holocene climate variability on the Kola Peninsula, Russian Subarctic, based on aquatic invertebrate records from lake sediments. *Quaternary Research 79*, 350–361.

Ingri, J., Pekka, L., Dauvalter, V., Rodushkin, I. & Peinerud, E. 2011: Manganese redox cycling in Lake Imandra: impact on nitrogen and

the trace metal sediment record. *Biogeosciences Discussions 8*, 273–321.

Innes, J. L. & Oleksyn, J. 1999: *Forest Dynamics in Heavily Polluted Regions*. 248 pp. CABI Publications, Wallingford.

Johansen, B. E., Karlsen, S. R. & Elvebakk, A. 2005: Monitoring vegetation changes on Finnmarksvidda, Northern Norway, using Landsat MSS and Landsat TM/ETM+ satellite images. *Phytocoenologia 35*, 969–984.

Jolliffe, I. T. 2002: *Principal Component Analysis*. 488 pp. Springer US, New York.

Jones, V. J., Leng, M. J., Solovieva, N., Sloane, H. J. & Tarasov, P. 2004: Holocene climate of the Kola Peninsula; evidence from the oxygen isotope record of diatom silica. *Quaternary Science Reviews 23*, 833–839.

Kagan, L. J., Koshechkin, B. I. & Lebedeva, R. M. 1992: Kol'skii poluostrov. *In* Davydova, N. N. (ed.): *Istoriya Ozer Vostochno Evropeiskoi Ravniny*, 20–34. Nauka, St. Petersburg.

Kalugin, I., Daryin, A., Smolyaninova, L., Andreev, A., Diekmann, B. & Khlystov, O. 2007: 800-yr-long records of annual air temperature and precipitation over southern Siberia inferred from Teletskoye Lake sediments. *Quaternary Research 67*, 400–410.

Karlsen, S. R., Elvebakk, A., Høgda, K. A. & Johansen, B. 2006: Satellite-based mapping of the growing season and bioclimatic zones in Fennoscandia. *Global Ecology and Biogeography 15*, 416–430.

Kattel, G. & Sirocko, F. 2011: Palaeocladocerans as indicators of environmental, cultural and archaeological developments in Eifel maar lakes region (West Germany) during the Lateglacial and Holocene periods. *Hydrobiologia 676*, 203–221.

Khromova, T., Nosenko, G., Kutuzov, S., Muraviev, A. & Chernova, L. 2014: Glacier area changes in Northern Eurasia. *Environmental Research Letters 9*, 015003, https://doi.org/10.1088/1748-9326/9/1/015003.

Kleman, J. & Glasser, N. F. 2007: The subglacial thermal organisation (STO) of ice sheets. *Quaternary Science Reviews 26*, 585–597.

Kleman, J. & Hättestrand, C. 1999: Frozen-bed Fennoscandian and Laurentide ice sheets during the Last Glacial Maximum. *Nature 402*, 63–66.

Kleman, J., Hättestrand, C., Borgström, I. & Stroeven, A. 1997: Fennoscandian palaeoglaciology reconstructed using a glacial geological inversion model. *Journal of Glaciology 43*, 283–299.

Koç, N., Jansen, E. & Haflidason, H. 1993: Paleoceanographic reconstructions of surface ocean conditions in the Greenland, Iceland and Norwegian seas through the last 14 ka based on diatoms. *Quaternary Science Reviews 12*, 115–140.

Kolka, V. V. & Korsakova, O. P. 2005: *Quaternary Geology and landforming processes.* International Field Symposium. 04-09 September 2005, Apatity, Kola Peninsula, Russia.

Kolka, V. V., Korsakova, O. P., Nikolaeva, S. B. & Yevzerov, V. 2008: *The Late Pleistocene interglacial, late glacial landforms and Holocene neotectonics of the Kola Peninsula.* Field Excursion. 33 IGC, The Nordic Countries. 14–23 August 2008, Apatity, Kola Peninsula, Russia.

Korhola, A. & Rautio, M. 2001: Cladocera and other branchiopod crustaceans. *In* Smol, J. P., Birks, H. J. B. & Last, W. M. (eds.): *Tracking Environmental Change Using Lake Sediments: Volume 4: Zoological Indicators*, 5–41. Springer Netherlands, Dordrecht.

Korhola, A. & Weckström, J. 2004: Paleolimnological studies in arctic Fennoscandia and the Kola Peninsula (Russia). *In* Smol, J. P., Pienitz, R. & Douglas, M. S. V. (eds.): *Long-term Environmental Change in Arctic and Antarctic Lakes*, 381–418. Springer Netherlands, Dordrecht.

Korsakova, O. P., Kolka, V. V., Tolstobrova, A. N., Lavrova, N. B., Tolstobrov, D. S. & Shelekhova, T. S. 2016: Lithology and late postglacial stratigraphy of bottom sediments in isolated basins of the White Sea coast exemplified by a small lake in the Chupa settlement area (Northern Karelia). *Stratigraphy and Geological Correlation 24*, 294–312.

Kotov, A. A., Sinev, A. Y., Glagolev, S. M. & Smirnov, N. N. 2010: Water fleas (Cladocera). *In* Alekseeva, V. R. & Calolihina, S. Y. (eds.): *Key Book for Zooplankton and Zoobenthos of Fresh Waters of European Russia*, 151–276. KMK, Moscow.

Kravtsova, V. 1995: Lake Imandra water contamination from space images. *In* Petts, G. E. (ed.): *Man's Influence on Freshwater Ecosystems and Water Use*, 67–72. The International Association of Hydrological Sciences, Colorado.

Kremenetski, C., Vaschalova, T. & Sulerzhitsky, L. 1999: The Holocene vegetation history of the Khibiny Mountains: implications for the post glacial expansion of spruce and alder on the Kola Peninsula, northwestern Russia. *Journal of Quaternary Science 14*, 29–43.

Kremenetski, K. V., MacDonald, G. M., Gervais, B. R., Borisova, O. K. & Snyder, J. A. 2004: Holocene vegetation history and climate change on the northern Kola Peninsula, Russia: a case study from a small tundra lake. *Quaternary International 122*, 57–68.

Kupriyanova, L. A. & Alyoshina, L. A. 1972: *Pollen and Spores of Plants from the Flora of European Part of USSR*. 170 pp. Academy of Sciences USSR, Komarov Botanical Institute, Leningrad (in Russian).

Kupriyanova, L. A. & Alyoshina, L. A. 1978: *Pollen and Spores of Plants from the Flora of European Part of USSR*. 184 pp. Academy of Sciences USSR, Komarov Botanical Institute, Leningrad (in Russian).

Kylander, M. E., Ampel, L., Wohlfarth, B. & Veres, D. 2011: High-resolution X-ray fluorescence core scanning analysis of Les Echets (France) sedimentary sequence: new insights from chemical proxies. *Journal of Quaternary Science 26*, 109–117.

Lebas, E., Krastel, S., Wagner, B., Gromig, R., Fedorov, G., Baumer, M., Kostromina, N. & Haflidason, H. 2019: Seismic stratigraphical record of Lake Levinson-Lessing, Taymyr Peninsula: evidence for ice-sheet dynamics and lake-level fluctuations since the Early Weichselian. *Boreas 48*, 470–487.

Leipe, T., Moros, M., Kotilainen, A., Vallius, H., Kabel, K., Endler, M. & Kowalski, N. 2013: Mercury in Baltic Sea sediments-Natural background and anthropogenic impact. *Chemie der Erde-Geochemistry 73*, 249–259.

Leng, M. J., Wagner, B., Anderson, N. J., Bennike, O., Woodley, E. & Kemp, S. J. 2012: Deglaciation and catchment ontogeny in coastal south-west Greenland: implications for terrestrial and aquatic carbon cycling. *Journal of Quaternary Science 27*, 575–584.

Lohne, Ø. S., Mangerud, J. & Birks, H. H. 2013: Precise ^{14}C ages of the Vedde and Saksunarvatn ashes and the Younger Dryas boundaries from western Norway and their comparison with the Greenland Ice Core (GICC05) chronology. *Journal of Quaternary Science 28*, 490–500.

Löwemark, L., Chen, H. F., Yang, T. N., Kylander, M., Yu, E. F., Hsu, Y. W., Lee, T. Q., Song, S. R. & Jarvis, S. 2011: Normalizing XRF-scanner data: a cautionary note on the interpretation of high-resolution records from organic-rich lakes. *Journal of Asian Earth Sciences 40*, 1250–1256.

Lukin, A. A. 2013: The present state of an Arctic charr (*Salvelinus alpinus* L.) population in Lake Imandra subjected to over-fishing. *Journal of Ichthyology 53*, 804–808.

Lundqvist, J. 1986: Late Weichselian glaciation and deglaciation in Scandinavia. *Quaternary Science Reviews 5*, 269–292.

Lundqvist, J. & Saarnisto, M. 1995: Summary of project IGCP-253. *Quaternary International 28*, 9–18.

MacDonald, G. M., Gervais, B. R., Snyder, J. A., Tarasov, G. A. & Borisova, O. K. 2000: Radiocarbon dated Pinus sylvestris L. wood from beyond tree-line on the Kola Peninsula, Russia. *The Holocene 10*, 143–147.

Mackereth, F. J. H. 1966: Some chemical observations on post-glacial lake sediments. *Philosophical Transactions of the Royal Society of London. Series B, Biological Sciences 250*, 165–213.

Magny, M., Begeot, C., Guiot, J. & Peyron, O. 2003: Contrasting patterns of hydrological changes in Europe in response to Holocene climate cooling phases. *Quaternary Science Reviews 22*, 1589–1596.

Malyasova, E. S., Monoszon, M. K. & Kalugina, L. V. 1973: O nakhodkakh pyl'tsy semeistva marevykh (Chenopodiaceae) v golotsenovykh osadkakh Kol'skogo poluostrova. *Vestnik Leningradskogo Universiteta, Geologiya Geographiya 12*, 155–167.

Malyasova, E. S., Yel'chaninova, E. M. & Vishnevskaya, E. M. 1974: Pyl'tsa i spory iz donnykh osadkov ozer tsentral'noi chasti Kol'skogo poluostrova i nekotorye voprosy paleogeografii golotsena etoi

territorii. *In* Forsh, L. F. & Nazarov, G. V. (eds.): *Ozera Razlichnykh Landshaftov Kol'skogo Poluostrova; Chast' 1, Gidrologoya Ozer i Kharakteristika Ikh Vodosborov*, 244–269. Izdatel'stvo Nauka, Leningrad.

Mangerud, J., Gyllencreutz, R., Lohne, Ø. & Svendsen, J. I. 2011: Glacial history of Norway. *In* Ehlers, J., Gibbard, P. L. & Hughes, P. D. (eds.): *Developments in Quaternary Sciences Chapter 22*, 279–298. Elsevier, Amsterdam.

Marshall, G. J., Vignols, R. M. & Rees, W. G. 2016: Climate change in the Kola Peninsula, Arctic Russia, during the last 50 years from meteorological observations. *Journal of Climate 29*, 6823–6840.

Mathisen, I. E., Mikheeva, A., Tutubalina, O. V., Aune, S. & Hofgaard, A. 2014: Fifty years of tree line change in the Khibiny Mountains, Russia: advantages of combined remote sensing and dendroecological approaches. *Applied Vegetation Science 17*, 6–16.

Mayer, L. M., Schick, L. L., Allison, M. A., Ruttenberg, K. C. & Bentley, S. J. 2007: Marine vs. terrigenous organic matter in Louisiana coastal sediments: the uses of bromine:organic carbon ratios. *Marine Chemistry 107*, 244–254.

Melles, M., Brigham-Grette, J., Minyuk, P. S., Nowaczyk, N. R., Wennrich, V., DeConto, R. M., Anderson, P. M., Andreev, A. A., Coletti, A., Cook, T. L., Haltia-Hovi, E., Kukkonen, M., Lozhkin, A. V., Rosen, P., Tarasov, P., Vogel, H. & Wagner, B. 2012: 2.8 million years of Arctic climate change from Lake El'gygytgyn, NE Russia. *Science 337*, 315–320.

Merkel, A. 2019: *Klimadaten für Städte weltweit*. Available at: https://de.climate-data.org/asien/russland/oblast-murmansk-608/ (accessed: 07.10.2019).

Meyer-Jacob, C., Bindler, R., Bigler, C., Leng, M. J., Lowick, S. E. & Vogel, H. 2017: Regional Holocene climate and landscape changes recorded in the large subarctic lake Torneträsk, N Fennoscandia. *Palaeogeography, Palaeoclimatology, Palaeoecology 487*, 1–14.

Meyers, P. A. & Ishiwatari, R. 1995: Organic matter accumulation records in lake sediments. *In* Lerman, A., Imboden, D. M. & Gat, J. R. (eds.): *Physics and Chemistry of Lakes*, 279–328. Springer Berlin, Heidelberg.

Mitrofanov, F. P. & Zozulya, D. R. 2002: *Major Geological Sights of the Kola Peninsula*. 160 pp. Russian Academy of Sciences, Kola Science Centre of RAS, Apatity.

Mitrofanov, F. P., Pozhilenko, V. I., Smolkin, V. F., Arzamastsev, A. A., Yakovlev, V. Y., Lyubtsov, V. V., Shipilov, E. V., Nikolaeva, S. B. & Fedotov, Z. A. 1995: *Geology of the Kola Peninsula*. 145 pp. Russian Academy of Sciences, Kola Science Centre of RAS, Apatity.

Mitrofanov, F. P., Radchenko, A. T., Klimov, S. A. & Gavrilenko, B. B. 2001: *Geological Map of the Kola Region*. Geological Institute of KSC RAS, Apatity.

Moiseenko, T. I. & Yakovlev, V. A. 1990: *Anthropogenic Modifications of Aquatic Systems of the Kola Arctic*. 224 pp. Nauka, Leningrad.

Moiseenko, T. I., Dauvalter, V. A., Lukin, A. A., Kudryavtseva, L. P., Iliachshuk, B. P., Iliachshuk, L. I., Sandimirov, S. S., Kagan, L., Vandysh, O. I., Sharov, A. N., Sharova, U. N. & Koroleva, I. N. 2002: *Anthropogenic Modification of Lake Imandra Ecosystem*. 403 pp. Nauka, Moscow.

Moiseenko, T. I., Dauvalter, V. & Rodushkin, I. 1996: *Geochemical Migration and Covariation of Elements in the Imandra Lake, Barents Region*. 103 pp. Kola Science Centre of the Russian Academy of Sciences, Apatity.

Moiseenko, T. I., Sharov, A. N., Vandish, O. I., Kudryavtseva, L. P., Gashkina, N. A. & Rose, C. 2009a: Long-term modification of Arctic lake ecosystems: Reference condition, degradation under toxic impacts and recovery (case study Imandra Lakes, Russia). *Limnologica 39*, 1–13.

Moiseenko, T. I., Gashkina, N. A., Sharov, A. N., Vandysh, O. I. & Kudryavtseva, L. P. 2009b: Anthropogenic transformations of the Arctic ecosystem of Lake Imandra: tendencies for recovery after long period of pollution. *Water Resources 36*, 296–309.

Moiseenko, T. I., Morgunov, B. A., Gashkina, N. A., Megorskiy, V. V. & Pesiakova, A. A. 2018: Ecosystem and human health assessment in relation to aquatic environment pollution by heavy metals: case study of the Murmansk region, northwest of the Kola Peninsula, Russia. *Environmental Research Letters 13*, 065005. https://doi.org/10.1088/1748-9326/aab5d2.

Moore, P. D., Webb, J. A. & Collison, M. E. 1991: *Pollen Analysis*. 216 pp. Blackwell Scientific Publications, Oxford.

Moros, M., Andersen, T. J., Schulz-Bull, D., Häusler, K., Bunke, D., Snowball, I., Kotilainen, A., Zillén, L., Jensen, J. B., Kabel, K., Hand, I., Leipe, T., Lougheed, B. C., Wagner, B. & Arz, H. W. 2017: Towards an event stratigraphy for Baltic Sea sediments deposited since AD 1900: approaches and challenges. *Boreas 46*, 129–142.

Müller, J., Oberhänsli, H., Melles, M., Schwab, M., Rachold, V. & Hubberten, H. W. 2001: Late Pliocene sedimentation in Lake Baikal: implications for climatic and tectonic change in SE Siberia. *Palaeogeography, Palaeoclimatology, Palaeoecology 174*, 305–326.

NASA/METI/AIST/Japan Spacesystems 2001: *ASTER Level 1A Data Set - Reconstructed, unprocessed instrument data (Data set). NASA EOSDIS Land Processes DAAC.* Available at: https://doi.org/10.5067/aster/ast_l1a.003 (accessed 19.12.2019).

NASA/METI/AIST/Japan Spacesystems 2019: *ASTER Global Water Bodies Database V001 (Data set). NASA EOSDIS Land Processes DAAC.* https://doi.org/10.5067/aster/astwbd.001 (accessed: 19.12.2019).

Nesje, A., Matthews, J. A., Dahl, S. O., Berrisford, M. S. & Andersson, C. 2001: Holocene glacier fluctuations of Flatebreen and winter-precipitation changes in the Jostedalsbreen region, western Norway, based on glaciolacustrine sediment records. *Holocene 11*, 267–280.

Nevalainen, L., Luoto, T. P., Kultti, S. & Sarmaja-Korjonen, K. 2013: Spatio-temporal distribution of sedimentary Cladocera (Crustacea: Branchiopoda) in relation to climate. *Journal of Biogeography 40*, 1548–1559.

Nevalainen, L., Rantala, M. V. & Luoto, T. P. 2015: Sedimentary cladoceran assemblages and their functional attributes record late Holocene climate variability in southern Finland. *Journal of Paleolimnology 54*, 239–252.

Niemela, J., Ekman, I. & Lukashov, A. V. 1993: *Quaternary Deposits of Finland and Northwestern Russia and their Metallogenic Potential*. MAP CENTER, Helsinki.

Nikolaeva, S. B., Lavrova, N. B., Tolstobrov, D. S. & Denisov, D. B. 2015: Reconstructions of Holocene paleogeographic conditions in the Lake Imandra area (Kola Peninsula): results of paleolimnological studies. *Proceedings of the Karelian Scientific Centre of RAS 5*, 30–47 (in Russian).

Ogureeva, G. N., Chernenkova, T. V., Puzachenko, M. J., Morozova, O. V., Tikhonova, E. V. & Kadetov, N. G. 2012: Modern vegetation mapping of the boreal forest biome of the Eastern European Russia. *Geobotanica - The East Asian Flora and its role in the formation of the world's vegetation,* 23–27 September 2012, Vladivostok.

Ojala, A. E. K., Alenius, T., Seppä, H. & Giesecke, T. 2008: Integrated varve and pollen-based temperature reconstruction from Finland: evidence for Holocene seasonal temperature patterns at high latitudes. *Holocene 18*, 529–538.

Olyunina, O. S., Polyakova, E. I. & Romanenko, F. A. 2008: Diatom assemblages from Holocene sediments of the Kola Peninsula. *Doklady Earth Sciences 423*, 1343–1347.

Orlova, M. A., Lukina, N. V., Tutubalina, O. V., Smirnov, V. E., Isaeva, L. G. & Hofgaard, A. 2012: Soil nutrient's spatial variability in forest–tundra ecotones on the Kola Peninsula, Russia. *Biogeochemistry 113*, 283–305.

Park, T., Ganguly, S., Tømmervik, H., Euskirchen, E. S., Högda, K. A., Karlsen, S. R., Brovkin, V., Nemani, R. R. & Myneni, R. B. 2016: Changes in growing season duration and productivity of northern vegetation inferred from long-term remote sensing data. *Environmental Research Letters 11*, 084001, https//doi.org/10.1088/1748-9326/11/8/084001.

Paterson, G. A., Heslop, D. & Pan, Y. X. 2016: The pseudo-Thellier palaeointensity method: new calibration and uncertainty estimates. *Geophysical Journal International 207*, 1596–1608.

Patton, H., Hubbard, A., Andreassen, K., Auriac, A., Whitehouse, P. L., Stroeven, A. P., Shackleton, C., Winsborrow, M., Heyman, J. & Hall, A. M. 2017: Deglaciation of the Eurasian ice sheet complex. *Quaternary Science Reviews 169*, 148–172.

Peck, J. A., King, J. W., Colman, S. M. & Kravchinsky, V. A. 1994: A rock-magnetic record from Lake Baikal, Siberia - evidence for Late Quaternary climate-change. *Earth and Planetary Science Letters 122*, 221–238.

Pripachkin, P. V., Neradovsky, Y. N., Fedotov, Z. A. & Nerovich, L. I. 2013: *The Cu-Ni-PGE and Cr deposits of the Monchegorsk area, Kola Peninsula, Russia.* 56 pp. IGC, The Nordic Countries. Geological Institute KSC RAS Press, 8-12 July 2013, Apatity.

Putkinen, N., Lunkka, J. P., Ojala, A. E. K. & Kosonen, E. 2011: Deglaciation history and age estimate of the Younger Dryas end moraines in the Kalevala region, NW Russia. *Quaternary Science Reviews 30*, 3812–3822.

R Development Core Team 2019: *A language and environment for statistical computing.* R Foundation for Statistical Computing, Vienna. Available at: https://www.R-project.org/.

Radchenko, A. T., Balagansky, V. V., Basalayev, A. A., Belyayev, O. A., Pozhilenko, V. I. & Radchenko, M. K. 1994: *An Explanatory Note on Geological Map of the North-Eastern Baltic Shield of a scale of 1:500000*. Kola Science Center of RAS, Apatity, 96 pp.

Rainio, H., Saarnisto, M. & Ekman, I. 1995: Younger-Dryas end moraines in Finland and NW Russia. *Quaternary International 28*, 179–192.

Rasmussen, S. O., Bigler, M., Blockley, S. P., Blunier, T., Buchardt, S. L., Clausen, H. B., Cvijanovic, I., Dahl-Jensen, D., Johnsen, S. J., Fischer, H., Gkinis, V., Guillevic, M., Hoek, W. Z., Lowe, J. J., Pedro, J. B., Popp, T., Seierstad, I. K., Steffensen, J. P., Svensson, A. M., Vallelonga, P., Vinther, B. M., Walker, M. J. C., Wheatley, J. J. & Winstrup, M. 2014: A stratigraphic framework for abrupt climatic changes during the Last Glacial period based on three synchronized Greenland ice-core records: refining and extending the INTIMATE event stratigraphy. *Quaternary Science Reviews 106*, 14–28.

Reimer, P. J., Bard, E., Bayliss, A., Beck, J. W., Blackwell, P. G., Ramsey, C. B., Brown, D. M., Buck, C. E., Edwards, R. L., Friedrich, M., Grootes, P. M., Guilderson, T. P., Haflidason, H., Hajdas, I., Hatté, C., Heaton, T. J., Hogg, A. G., Hughen, K. A., Kaiser, K. F., Kromer, B., Manning, S. W., Reimer, R. W., Richards, D. A., Scott, E. M., Southon, J. R., Turney, C. S. M. & van der Plicht, J. 2013a: Selection and treatment of data for radiocarbon calibration: an update to the international calibration (Intcal) criteria. *Radiocarbon 55*, 1923–1945.

Reimer, P. J., Bard, E., Bayliss, A., Beck, J. W., Blackwell, P. G., Ramsey, C. B., Buck, C. E., Cheng, H., Edwards, R. L., Friedrich, M., Grootes, P. M., Guilderson, T. P., Haflidason, H., Hajdas, I., Hatté, C., Heaton, T. J., Hoffmann, D. L., Hogg, A. G., Hughen, K. A., Kaiser, K. F., Kromer, B., Manning, S. W., Niu, M., Reimer, R. W., Richards, D. A., Scott, E. M., Southon, J. R., Staff, R. A., Turney, C. S. M. & van der Plicht, J. 2013b: Intcal13 and Marine13 radiocarbon age calibration curves 0-50,000 years cal BP. *Radiocarbon 55*, 1869–1887.

Renberg, I. 1985: Influences of acidification on the sediment chemistry of Lake Gårdsjön, SW Sweden. *Ecological Bulletins 37*, 246–250.

Rethemeyer, J., Fülop, R. H., Höfle, S., Wacker, L., Heinze, S., Hajdas, I., Patt, U., König, S., Stapper, B. & Dewald, A. 2013: Status report on sample preparation facilities for C-14 analysis at the new CologneAMS center. *Nuclear Instruments & Methods in Physics Research Section B-Beam Interactions with Materials and Atoms 294*, 168–172.

Reynolds, R. L., Rosenbaum, J. G., Rapp, J., Kerwin, M. W., Platt Bradbury, J., Colman, S. & Adam, D. 2004: Record of Late Pleistocene glaciation and deglaciation in the southern Cascade Range. I. Petrological evidence from lacustrine sediment in Upper Klamath Lake, Southern Oregon. *Journal of Paleolimnology 31*, 217–233.

Rigina, O. 2002: Environmental impact assessment of the mining and concentration activities in the Kola Peninsula, Russia by multidate remote sensing. *Environmental Monitoring and Assessment 75*, 11–31.

Rigina, O. & Kozlov, M. V. 2000: The impacts of air pollution on the northern taiga forests of the Kola Peninsula, Russian Federation. *In* Innes, J. L. (ed.): *Forest dynamics in heavily polluted regions. Report No. 1 of the IUFRO Task Force on Environmental Change*, 37–65. CABI Publications, Wallingford.

Rohling, E. J. & Pälike, H. 2005: Centennial-scale climate cooling with a sudden cold event around 8,200 years ago. *Nature 434*, 975–979.

Rubel, F. & Kottek, M. 2010: Observed and projected climate shifts 1901-2100 depicted by world maps of the Köppen-Geiger climate classification. *Meteorologische Zeitschrift 19*, 135–141.

Rumyantsev, V. A., Drabkova, V. G. & Izmailova, A. V. 2012: *The Great Lakes of the World*. 370 pp. Lema, St. Petersburg (in Russian).

Rzevsky, B. N. 1997: *Dictionary of Saami Geographical Terms of Khibiny.* 27 pp. Golos Prirody, Kirovsk.

Salonen, J. S., Seppä, H., Väliranta, M., Jones, V. J., Self, A., Heikkilä, M., Kultti, S. & Yang, H. 2011: The Holocene thermal maximum and late-Holocene cooling in the tundra of NE European Russia. *Quaternary Research 75*, 501–511.

Sarmaja-Korjonen, K. 2002: Multi-proxy data from Kaksoislammi Lake in Finland: dramatic changes in the late Holocene cladoceran assemblages. *Journal of Paleolimnology 28*, 287–296.

Sarmaja-Korjonen, K., Szeroczynska, K. & Gasiorowski, M. 2003: Subfossil chydorid taxa and assemblages from lake sediments in Poland and Finland with special reference to climate. *Studia Quaternaria 20*, 25–34.

Sauerbrey, M. A., Juschus, O., Gebhardt, A. C., Wennrich, V., Nowaczyk, N. R. & Melles, M. 2013: Mass movement deposits in the 3.6Ma sediment record of Lake El'gygytgyn, Far East Russian Arctic. *Climate of the Past 9*, 1949–1967.

Savelieva, L., Raschke, E. & Titova, D. 2013: *Photographic Atlas of Plants and Pollen of the Lena River Delta*. 113 pp. SPbGU, Saint-Petersburg (in Russian).

Savelieva, L. A., Andreev, A. A., Gromig, R., Subetto, D. A., Fedorov, G. B., Wennrich, V., Wagner, B. & Melles, M. 2019: Vegetation and climate changes in northwestern Russia during the Lateglacial and Holocene inferred from the Lake Ladoga pollen record. *Boreas 48*, 349–360.

Seppä, H. & Birks, H. J. B. 2001: July mean temperature and annual precipitation trends during the Holocene in the Fennoscandian tree-line area: pollen-based climate reconstructions. *The Holocene 11*, 527–539.

Seppä, H. & Birks, H. J. B. 2002: Holocene climate reconstructions from the Fennoscandian tree-line area based on pollen data from Toskaljavri. *Quaternary Research 57*, 191–199.

Seppä, H., Birks, H. J. B., Giesecke, T., Hammarlund, D., Alenius, T., Antonsson, K., Bjune, A. E., Heikkilä, M., MacDonald, G. M., Ojala, A. E. K., Telford, R. J. & Veski, S. 2007: Spatial structure of the 8200 cal yr BP event in northern Europe. *Climate of the Past 3*, 225–236.

Shilova, O. S., Romanenko, F. A., Kolka, V. V. & Denisov, D. B. 2019: Holocene environmental changes in the Northern Khibiny mountains (Kola Peninsula) inferred by diatom analysis of lake sediments. *Geomorphology RAS 2019*, 91–101 (in Russian).

Shvarev, S. V. 2003: Postglacial tectonic movements and formation of the Imandra lake terraces (the Kola Peninsula). *Geomorfologiya 4*, 97–105 (in Russian).

Silliman, J. E., Meyers, P. A. & Bourbonniere, R. A. 1996: Record of postglacial organic matter delivery and burial in sediments of Lake Ontario. *Organic Geochemistry 24*, 463–472.

Slabunov, A. I., Lobach-Zhuchenko, S. B., Bibikova, E. V., Balagansky, V. V., Sorjonen-Ward, P., Volodichev, O. I., Shchipansky, A. A., Svetov, S. A., Chekulaev, V. P., Arestova, N. A. & Stepanov, V. S. 2006: The Archean of the Baltic Shield: Geology, geochronology, and geodynamic settings. *Geotectonics 40*, 409–433.

Snowball, I. & Sandgren, P. 1996: Lake sediment studies of Holocene glacial activity in the Karsa valley, northern Sweden: contrasts in interpretation. *Holocene 6*, 367–372.

Snyder, J. A., Forman, S. L., Mode, W. N. & Tarasov, G. A. 1997: Postglacial relative sea-level history: sediment and diatom records of emerged coastal lakes, north-central Kola Peninsula, Russia. *Boreas 26*, 329–346.

Snyder, J. A., Macdonald, G. M., Forman, S. L., Tarasov, G. A. & Mode, W. N. 2000: Postglacial climate and vegetation history, north-central Kola Peninsula, Russia: pollen and diatom records from Lake Yarnyshnoe-3. *Boreas 29*, 261–271.

Solovieva, N. & Jones, V. J. 2002: A multiproxy record of Holocene environmental changes in the central Kola Peninsula, northwest Russia. *Journal of Quaternary Science 17*, 303–318.

Solovieva, N., Tarasov, P. E. & MacDonald, G. 2005: Quantitative reconstruction of Holocene climate from the Chuna Lake pollen record, Kola Peninsula, northwest Russia. *The Holocene 15*, 141–148.

St. Amour, N. A., Hammarlund, D., Edwards, T. W. D. & Wolfe, B. B. 2010: New insights into Holocene atmospheric circulation dynamics in central Scandinavia inferred from oxygen-isotope records of lake-sediment cellulose. *Boreas 39*, 770–782.

Stockmarr, J. A. 1971: Tablets with spores used in absolute pollen analysis. *Pollen et Spores 13*, 615–621.

Stroeven, A. P., Hättestrand, C., Kleman, J., Heyman, J., Fabel, D., Fredin, O., Goodfellow, B. W., Harbor, J. M., Jansen, J. D., Olsen, L., Caffee, M. W., Fink, D., Lundqvist, J., Rosqvist, G. C., Strömberg, B. & Jansson, K. N. 2016: Deglaciation of Fennoscandia. *Quaternary Science Reviews 147*, 91–121.

Svendsen, J. I., Alexanderson, H., Astakhov, V. I., Demidov, I., Dowdeswell, J. A., Funder, S., Gataullin, V., Henriksen, M., Hjort, C., Houmark-Nielsen, M., Hubberten, H. W., Ingólfsson, Ó., Jakobsson, M., Kjær, K. H., Larsen, E., Lokrantz, H., Lunkka, J. P., Lysså, A., Mangerud, J., Matiouchkov, A., Murray, A., Möller, P., Niessen, F., Nikolskaya, O., Polyak, L., Saarnisto, M., Siegert, C., Siegert, M. J., Spielhagen, R. F. & Stein, R. 2004: Late Quaternary ice sheet history of northern Eurasia. *Quaternary Science Reviews 23*, 1229–1271.

Szeroczyńska, K. & Sarmaja-Korjonen, K. 2007: *Atlas of Subfossil Cladocera from Central and Northern Europe*. 84 pp. Friends of the Lower Vistula Society, Świecie.

The MathWorks Inc. 2019: *MATLAB version 9.6.0.1072779 (R2019a)*. The MathWorks Inc., Natick.

Tjallingii, R., Röhl, U., Kölling, M. & Bickert, T. 2007: Influence of the water content on X-ray fluorescence core-scanning measurements in soft marine sediments. *Geochemistry, Geophysics, Geosystems 8*, Q02004, https://doi.org/10.1029/2006GC001393.

Tolstobrova, A., Tolstobrov, D., Kolka, V. & Korsakova, O. 2016: Late glacial and postglacial history of Lake Osinovoye (Kola region) inferred from sedimentary diatom assemblages. *Proceedings of the Karelian Research Centre of the Russian Academy of Sciences 5*, 106–116 (in Russian).

Valiranta, M., Weckstrom, J., Siitonen, S., Seppä, H., Alkio, J., Juutinen, S. & Tuittila, E. S. 2011: Holocene aquatic ecosystem change in the boreal vegetation zone of northern Finland. *Journal of Paleolimnology 45*, 339–352.

Vasilevskaya, N. V. 2014: *Ecology of Plants of the Arctic*. 184 pp. Murmansk State Humanities University, Murmansk (in Russian).

Voinov, A., Bromley, L., Kirk, E., Korchak, A., Farley, J., Moiseenko, T., Krasovskaya, T., Makarova, Z., Megorski, V., Selin, V., Kharitonova, G. & Edson, R. 2004: Understanding human and ecosystem dynamics in the Kola Arctic: a participatory integrated study. *Arctic 57*, 375–388.

Walker, M., Johnsen, S., Rasmussen, S. O., Popp, T., Steffensen, J.-P., Gibbard, P., Hoek, W., Lowe, J., Andrews, J., Björck, S., Cwynar, L. C., Hughen, K., Kershaw, P., Kromer, B., Litt, T., Lowe, D. J., Nakagawa, T., Newnham, R. & Schwander, J. 2009: Formal definition and dating of the GSSP (Global Stratotype Section and Point) for the base of the Holocene using the Greenland NGRIP ice core, and selected auxiliary records. *Journal of Quaternary Science 24*, 3–17.

Wanner, H., Beer, J., Bütikofer, J., Crowley, T. J., Cubasch, U., Flückiger, J., Goosse, H., Grosjean, M., Joos, F., Kaplan, J. O., Küttel, M., Müller, S. A., Prentice, I. C., Solomina, O., Stocker, T. F., Tarasov, P., Wagner, M. & Widmann, M. 2008: Mid- to Late Holocene climate change: an overview. *Quaternary Science Reviews 27*, 1791–1828.

Weckstrom, J., Seppä, H. & Korhola, A. 2010: Climatic influence on peatland formation and lateral expansion in sub-arctic Fennoscandia. *Boreas 39*, 761–769.

Whiteside, M. C. 1970: Danish Chydorid Cladocera - modern ecology and core studies. *Ecological Monographs 40*, 79–118.

Williams, P. F. & Rust, B. R. 1969: The sedimentology of a braided river. *Journal of Sedimentary Research 39*, 649–679.

Wohlfarth, B., Schwark, L., Bennike, O., Filimonova, L., Tarasov, P., Björkman, L., Brunnberg, L., Demidov, I. & Possnert, G. 2004: Unstable early-Holocene climatic and environmental conditions in northwestern Russia derived from a multidisciplinary study of a lake-sediment sequence from Pichozero, southeastern Russian Karelia. *Holocene 14*, 732–746.

Yevzerov, V. Y. & Nikolaeva, S. B. 2008: Terminal stages of the evolution of sheet and mountain glaciations in Khibiny. *Doklady Earth Sciences 421*, 792–795.

Yu, Z. C. & Wright, H. E. 2001: Response of interior North America to abrupt climate oscillations in the North Atlantic region during the last deglaciation. *Earth-Science Reviews 52*, 333–369.

Ziegler, M., Jilbert, T., de Lange, G. J., Lourens, L. J. & Reichart, G.-J. 2008: Bromine counts from XRF scanning as an estimate of the marine organic carbon content of sediment cores. *Geochemistry, Geophysics, Geosystems 9*, Q05009. https://doi.org/10.1029/2007GC001932.

Zitko, V. 1994: Principal component analysis in the evaluation of environmental data. *Marine Pollution Bulletin 28*, 718–722.

Zyuzin, Y. L. & Demin, V. I. 2007: Climate of the Khibiny Mountains *International Conference on Alpine Meteorology*. Meteo France, 4.-8. June 2007, Chambery.